

Assessment of the potential role of PM_{2.5}/PM₁₀ particles in intensifying the pandemic spread of SARS-CoV-2/COVID-19 in Northern Italy

Paolo Di Girolamo (✉ paolo.digirolamo@unibas.it)

Scuola di Ingegneria, Università degli Studi della Basilicata <https://orcid.org/0000-0002-7420-3164>

Research Article

Keywords: COVID-19, SARS-CoV-2, Environmental pollution, PM_{2.5}, PM₁₀, Epidemiologic parameters, Virus airborne transmission.

Posted Date: September 3rd, 2020

DOI: <https://doi.org/10.21203/rs.3.rs-67436/v1>

License:  This work is licensed under a Creative Commons Attribution 4.0 International License.

[Read Full License](#)

Abstract

The Severe Acute Respiratory Syndrome CoronaVirus 2 (SARS-CoV-2), which exploded in Wuhan (Hebei Region, China) in late 2019, has recently spread around the World, causing pandemic effects on humans. Italy, and especially its Northern regions around the Po Valley, has been facing severe effects in terms of infected individuals and casualties (more than 31.000 deaths and 255.000 infected people by mid-May 2020). While the spread and effective impact of the virus is primarily related to the life styles and social habits of the different human communities, environmental and meteorological factors also play a role. Among these, pollution from PM2.5/PM10 particles, which may directly impact on the human respiratory system or act as virus carrier, thus behaving as potential amplifying factors in the pandemic spread of SARS-CoV-2. Enhanced levels of PM2.5/PM10 particles in Northern Italy were observed over the two month period preceding the virus pandemic spread. Threshold levels for PM10 ($<50 \mu\text{g}/\text{m}^3$) were exceeded on 20-35 days over the period January-February 2020 in many areas in the Po Valley, where major effects in terms of infections and casualties occurred, with levels in excess of $80 \mu\text{g}/\text{m}^3$ occasionally observed in the 1-3 weeks preceding the contagious activation around February 25th. Threshold values for PM2.5 indicated in WHO air quality guidelines ($<25 \mu\text{g}/\text{m}^3$) were exceeded on more than 40 days over the period January-February 2020 in large portions of the Po Valley, with levels up to $70 \mu\text{g}/\text{m}^3$ observed in the weeks preceding the contagious activation. The evolution of particle matter concentration levels throughout the month of February 2020 was carefully monitored and results are reported in the paper.

In this paper PM10 particle measurements are compared with epidemiologic parameters data. Specifically, a statistical analysis is carried out to correlate the infection rate, or incidence of the pathology, the mortality rate and the case fatality rate with PM concentration levels. The study considers epidemiologic data for all 110 Italian Provinces, as reported by the Italian Statistics Institute (ISTAT, 2020), over the period 20 February-31 March 2020. Corresponding PM10 concentration levels were collected from the network of air quality monitoring stations run by different Regional and Provincial Environment Agencies, covering the period 15-26 February 2020. The case fatality rate is found to be highly correlated to the average PM10 concentration, with a correlation coefficient of 0.89 and a slope of the regression line of $(6.7 \pm 0.3) \times 10^{-3} \text{ m}^3/\mu\text{g}$, which implies a doubling (from 3 to 6 %) of the mortality rate of infected patients for an average PM10 concentration increase from 22 to 27 $\mu\text{g}/\text{m}^3$. Infection and mortality rates are also found to be correlated with PM10 concentration levels, with correlation coefficients being 0.82 and 0.80, respectively, and the slopes of the regression lines indicating a doubling (from 1 to 2 ‰) of the infection rate and a tripling (from 0.1 to 0.3 ‰) of the mortality rate for an average PM10 concentration increase from 25 to 29 $\mu\text{g}/\text{m}^3$. Epidemiologic parameters data were also compared with population density data, but no clear evidence of a mutual correlation between these quantities was found. Considerations on the exhaled particles' sizes and concentrations, their residence times, transported viral dose and minimum infective dose, in combination with PM2.5/PM10 pollution measurements and an analytical microphysical model, allowed assessing the potential role of airborne

transmission through virus-transmitting PM particles, in addition to droplet transmission, in conveying SARS-CoV-2 in the human respiratory system.

Introduction And Methods

PM_{2.5}/PM₁₀ are pollution particles with an aerodynamic radius of less than 2.5 and 10 μm, respectively, which are often present in the air. These small particles can be either organic or inorganic and can be present in both the solid and liquid phase. They are capable of adsorbing on their surface various substances with toxic properties such as sulphates, nitrates, metals and volatile compounds.

Suspended PM_{2.5}/PM₁₀ particles have been demonstrated to have a significant impact on human health, the higher being their concentration, the greater being their health impact (among others, Dockery et al., 1993; Pope et al., 1995; Brunekreef, 1997; Hoek et al., 2002). More specifically, atmospheric aerosols have been demonstrated to play an important role in triggering pro- inflammation and oxidation mechanisms of the lungs. Prolonged exposure to PM_{2.5}/PM₁₀ has been found to be linked to acute respiratory inflammation and immunological alterations (among others, Li et al., 2018, Losacco and Perillo, 2018). Recent studies and field measurements have also demonstrated that aerosols can represent an important vehicle for virus transmission (Sattar and Ijaz 1987; Fabian et al. 2008; Tellier 2009).

In the present paper we report a statistical analysis correlating SARS-CoV-2/COVID-19 epidemiologic parameters to PM₁₀ particle concentration measurements. In a recent paper by Borro et al. (2020), the variability of the infection rate, the mortality rate and the case fatality rate as a function of particle concentration was estimated for PM_{2.5} particles only, recognizing a primary role of these smaller particles in inducing an over-expression of the angiotensin conversion enzyme 2 (ACE-2) in the human respiratory system (among others, see papers by Gemmati et al., 2020; Devaux et al., 2020; Bunyavanich et al., 2020; Leung et al., 2020), and consequently in enhancing COVID-19 epidemiologic impact. In the present paper we extend the analysis to PM₁₀ particles.

Furthermore, in the study by Borro et al. (2020) particulate matter measurements from a single station for each province were considered, while in the present study we consider measurements from all ground stations present within each province territory, which allows to account for the natural variability of the particulate loading within the single province territories, including urban, semi-urban and rural areas. In fact, particulate concentration variability within each province territory may be large; this variability may severely affect the correlation between epidemiologic parameters and atmospheric pollution and needs to be properly accounted for. For this purpose, particulate concentration variability within each Province territory is used in the present paper as a weighting factor in the statistical analysis correlating epidemiologic factors with PM₁₀ concentration levels.

The paper outline is the following. Section 2 shortly describes compositional, size and microphysical properties of PM_{2.5}/PM₁₀ particles. Section 3 illustrates the possible interaction mechanisms of aerosol particles with the human respiratory system. Section 4 provides an assessment of the potential role of

airborne transmission. Section 5 illustrates the different datasets and sensors used in the study. Section 6 illustrates the achieved results in terms of the characterization of the evolution of PM_{2.5}/PM₁₀ concentration levels shortly before the pandemic outbreak; results in terms of correlations between epidemiologic parameters and PM concentration levels are also illustrated in this section. Finally, section 7 provides a summary of all results and some perspectives on possible future continuations of this research effort.

2. PM_{2.5}/PM₁₀ particles: their origin, composition, size and microphysical properties and residence times

Most atmospheric PM_{2.5}/PM₁₀ sources in polluted environments are linked to human activities. Generally, PM_{2.5} particles are formed from high temperature processes, such as vehicular exhaust, oil and coal combustion processes (internal combustion engines, heating systems, industrial activities, incinerators and thermoelectric power plants, biomass burning), industrial processes and chemical reactions in the atmosphere (Harrison et al., 2003; Samara et al., 2003). In general, the higher the combustion temperatures, the smaller are the emitted particles. These particles are harmful because of their small sizes and their capability to adsorb toxic combustion residues, such as polycyclic hydrocarbons, polychlorinated biphenyls, benzene, heavy metals and dioxins, which can potentially accumulate in living organisms. PM₁₀ particles are generally generated through attrition processes, including mechanical abrasion of crustal material and re-suspension of road and soil dust, sea spray, volcanic eruptions and brake and tire wear from vehicles (Allen et al., 2001). The above mentioned sources are primary sources for PM_{2.5}/PM₁₀ particles. Black carbon, which is essentially soot, and soil are the main components of these sources. PM_{2.5}/PM₁₀ concentration levels in urban areas drastically increase in the autumn-winter period as a result of the intensification of vehicular mobility and particle emissions from heating systems, in particular those powered with wood biomasses. Furthermore, winter meteorological conditions may favor an accumulation of PM particles because of occurrence of favorable atmospheric conditions, such as thermal inversions, which prevent particle dispersion and can cause particle accumulation in the lowest atmospheric levels.

A recent study on pollution in the Lombardy region (Northern Italy), an area where the maximum permitted PM₁₀ concentration threshold is frequently exceeded, revealed that the primary sources of PM₁₀ particles are wood biomass combustion (pellet or wood stoves), responsible for 45% of the particles present in the air, diesel engines, contributing with 14%, while 13% results from particles detaching from brake pads and tires (ARPA Lombardia, 2017). Another important source of PM_{2.5}/PM₁₀ particles in this region is represented by the degradation of road surface asphalt.

Secondary aerosol formation, together with long-range atmosphere transport, represents an additional important source for PM_{2.5}/PM₁₀ particles. Secondary components contribute to the formation of PM_{2.5} particles through chemical reaction, coagulation and other mechanisms. Ammonia (NH₃) and inorganic acid gases emitted from agricultural activities, livestock and poultry operations and manure treatment, handling and application, in combination with NO_x and VOC compounds, can affect air quality through the formation of secondary PM_{2.5}/PM₁₀ particles. High ammonia emissions, especially from agriculture and livestock husbandry, take place over extended areas in the Po Valley. Compared to the winter season, photochemical formation of secondary aerosol intensifies during spring with the intensification of solar radiation and the increase of surface temperatures, ultimately affecting air quality.

Composition analyses carried out on PM_{2.5}/PM₁₀ particles in different polluted regions of the globe have revealed that the percentage of the PM_{2.5} particles formed through secondary aerosol formation from secondary components (sulfates, nitrates, ammonium, organic carbon) varies anywhere from 30 to 90% (among others, Hodan et al., 2004, Kumar and Sunder Raman, 2016; Ram and Sarin, 2011; Rastogi et al., 2016). More specifically, the percentage of PM_{2.5} particles formed from VOC precursors (among others, formaldehyde - HCHO) is found to vary from 11% to 41%, and the percentage of PM_{2.5} formed from NO_x precursors varies from 4% to 37% (Hodan and Barnard, 2004).

The definition of PM_{2.5} and PM₁₀ as pollution particles having an aerodynamic radius smaller than 2.5 and 10 μm, respectively, provides an upper size limit for particle dimensions, but does not provide any information of particle size distribution. PM_{2.5} and PM₁₀ measurements are typically carried out with filtration samplers equipped with size-selective inlets capable to discriminate particles smaller than 2.5 and 10 μm, respectively. Particle number, volume and mass concentration varies as a function of the radius and a comprehensive evaluation on the potential impact of these particles on human health requires an accurate assessment of their size distributions. While information on particle size distribution cannot be inferred from filter based samples, several literature papers indicate PM mass distributions in urban background conditions having a predominance of fine particle (PM_{2.5}) mass, whereas industrial areas are typically dominated by the coarse fraction (PM_{2.5-10}) (among others, Taiwo et al., 2014; Pandolfi et al., 2011), with particle size distributions often found to be bimodal (Seinfeld and Pandis, 1998; Verrilli et al., 2010).

The potential effects of suspended PM particles on human health is strongly dependent on their life time, or residence time, in the air. Atmospheric residence time of PM particles is primarily dependent on their sizes and on atmospheric conditions. Vecchi et al. (2007) reported a residence time for atmospheric PM₁₀ particles in Milan of 10-12 h, while finer aerosols' residence time was estimated to be in the range 18–38 h (Vecchi et al., 2005).

3. Considerations on inhaled aerosol particles and their potential interaction with the human respiratory system

Suspended aerosol particles have been demonstrated to have a significant impact on human health, the higher being their concentration, the greater being their health effect (among others, Dockery et al., 1993; Pope et al., 1995; Brunekreef, 1997; Hoek et al., 2002). More specifically, atmospheric aerosols were demonstrated to play an important role in triggering pro-inflammation and oxidation processes in the lungs. Prolonged exposure to PM_{2.5}/PM₁₀ has been found to induce acute respiratory inflammation and immunological alterations (among others, Gemmati et al., 2020; Leung et al., 2020). A mortality analysis carried out by Cui et al. (2003) for the previous coronavirus SARS (SARS-CoV-1) in China pointed out that patients in regions with moderated air pollution levels were more likely to die than those living in regions with low air pollution levels.

High concentrations of PM particles have been documented to lead to an over-expression of the viral receptor ACE-2 in the human respiratory system (among others, see papers by Borro et al., 2020; Gemmati et al., 2020; Devaux et al., 2020; Bunyavanich et al., 2020; Leung et al., 2020). It was speculated that the presence of an elevated number of viral receptors in the host cells may increase the susceptibility to SARS-CoV-2 infection. Thus, pollution-induced over-expression of ACE-2 on human airways may favor SARS-CoV-2 infectivity.

Recent studies and field measurements have also demonstrated that aerosols represent an important vehicle for virus transmission (Sattar and Ijaz 1987; Fabian et al. 2008; Tellier 2009). In order for virus transmission through aerosols to occur, with PM particles acting as virus carriers, particles must carry a sufficient amount of the infectious virus and the virus must survive and remain infectious in the carrier particle for a sufficiently long time before it reaches a susceptible host cell and initiate infection. In general, airborne infectious viruses are difficult to monitor due to their extremely low concentration in air and because of the inadequacy and lack of accuracy of currently used air samplers. Despite these difficulties, the presence of SARS-CoV-2 was successfully detected on PM₁₀ particles in a polluted area in Northern Italy in the period 21 February – 13 March 2020 (Setti et al., 2020), i.e. at the time of the pandemic outbreak. Measurements of PM₁₀ particles reported by these authors were carried out with a low-volume gravimetric air sampler using quartz fiber filters. In this work the presence of SARS-CoV-2 viral RNA was revealed through the detection of the highly specific “RtDR gene” on 8 filters out of 34 samples in outdoor PM₁₀ pollution samples. However, these measurements did not allow to assess whether the virus amount was sufficiently high to induce infection. At present, there is no clear and univocal assessment of the aerosol viral load and the minimum infectious dose which is necessary in order for COVID-19 to be transmitted, although previous studies focusing on other viral respiratory pathologies indicated that very low virus loads can initiate infection (Nicas et al., 2005).

The primary vehicle of virus transmission is represented by droplet transmission. This is because, in case of coughing or sneezing, small liquid droplets, which may contain an infective amount of virus, are sprayed from the nose or the mouth. In order to avoid risks of infection through sneezing and coughing, the World Health Organization has advised to maintain at least one meter distance between individuals (WHO, 2020a). However, this recommendation does not take into account the potential role of atmospheric particles as virus carriers, i.e. airborne transmission.

To better address this point, it is to be pointed out that coughs and sneezes are capable to primarily spread droplets of saliva and mucus (droplet transmission), these particles being assumed to be typically larger than 5 μm . More specifically, Xie et al. (2007) determined that droplets emitted during coughing with sizes in the range 60–100 μm would fall to the ground within 2 m, while smaller size droplets produced during sneezing can travel more than 6 m away. However, particles smaller than 5 μm are also exhaled during coughing and sneezing (Lindsley et al., 2010; Fabian et al., 2011). Additionally, as previously anticipated, airborne transmission is also possible, which relies on tinier particles, possibly produced by talking or even breathing (Duguid 1946; Papineni and Rosenthal 1997). These latter particles have a longer atmospheric residence time and can travel further. Airborne transmission is more likely to characterize symptomless infected patients. At present, there are no studies in the open scientific literature specifically reporting on the analysis of cough and breath samplings from patients infected with SARS-CoV-2/COVID-19, but SARS-CoV-2 has been detected in the air indoor samples in hospitals (Liu et al., 2020; Santarpia et al., 2020). The World Health Organization has recently acknowledged the emerging evidence that SARS-CoV-2/COVID-19 can be spread by tiny particles suspended in the air, thus recognizing that the inhalation of aerosol particles containing a sufficient virus quantity can cause infection within the recipient (WHO, 2020b).

Exhaled breath particles produced by humans have sizes and numbers which depend on their respiratory patterns (Morawska et al., 2009). Sizes and concentrations of particles exhaled during talking or breathing have been measured by a variety of authors. More specifically, Wan et al. (2014) reported sizes smaller than 5 μm , with 80% of them in the range from 0.3 to 1.0 μm . Fairchild and Stampfer (1987) observed particles between 0.1 and 3 μm exhaled during nose and mouth breathing, and reported a geometric mean concentration of 230 particles per liter during tidal breathing, with more than 98% of the measured particles having sizes smaller than 1 μm . Papineni et al. (1997) measured particles with sizes between 0.3 and 8.0 μm exhaled during mouth and nose breathing and found that more than 84% of these particles were smaller than 1 μm . In this regard it is to be specified that the sizes of viruses are much smaller, typically ranging from 70 to 90 nm (Kim et al., 2020). Morawska et al. (2009) demonstrated that vocalization emits up to an order of magnitude more aerosol particles than breathing, with the number of produced aerosols increasing with increasing speaking volume (Asadi et al. (2019)). Furthermore, suspended microscopic aerosol particles may also consist of residual solid components of evaporated respiratory droplets, which are even tinier and may remain suspended longer (Asadi et al., 2020). Gralton et al. (2013), while focusing on influenza virus, respiratory syncytial virus and human metapneumovirus and rhinoviruses, determined that, when breathing, 58% of their infected patients produced large particles (>5 μm) containing viral RNA, while 80% produced small particles (<5 μm)

carrying viral RNA. The same authors determines that, when coughing, 57% of their infected patients produced large particles containing viral RNA, while 82% produced small particles containing viral RNA.

In the evaluation of the potential role of atmospheric aerosols as virus carriers, the capability of atmospheric particles to incorporate small potentially infectious droplets produced during breathing or speaking viruses has to be properly assessed. The primary process allowing atmospheric particles (PM_{2.5}/PM₁₀) to incorporate tiny infectious droplets (1mm or smaller) is represented by coagulation. In a coagulation process two particles collide and eventually adhere, or coalesce, with three fundamental mechanisms potentially determining particles' collisions: i.e. Brownian diffusion, turbulent fluctuations and particle differential vertical velocity. As a result of coagulation, a larger particle is created from two smaller particles. Consequently, coagulation leads to a reduction in the number of particles and an increase in their sizes (Smoluchowski, 1916, 1918). Eventually, small particles emitted during breathing or speaking, each one carrying a limited virus infective amount, may colloid and coalesce with suspended PM particles, eventually leading to PM particles carrying a sufficient virus amount for the infection to be transmitted. Infected PM particles can remain suspended in the air for hours and travel over much longer distances than the large particles emitted during coughing or sneezing, ultimately entering the human respiratory system.

The effectiveness of airborne transmission strongly depends on SARS-CoV-2 infectious dose. The infectious dose represents the virus amount needed to initiate an infection. Depending on the virus, people need to be exposed to as little as 10 virus particles – for example, for influenza viruses – or as many as thousands for other human viruses to get infected (Lakdawala and Gaglia, 2020). However, the number of SARS-CoV-2 viruses needed to trigger COVID-19 infection is not known yet and represents an important topic for scientific investigation. The intense worldwide pandemic outbreak of COVID-19 clearly testifies that SARS-CoV-2 is very contagious, but this may indicate either that a limited number of viruses are needed for infection (low infectious dose) or that infected people release a lot of viruses in the external environment.

The incorporation of viruses by atmospheric particles through coagulation is a process with a high efficiency variability. SARS-CoV-2 stability in aerosols was recently estimated by van Doremalen et al. (2020), who determined virus decay rates using a Bayesian regression model. Results from these authors indicate that SARS-CoV-2 remains viable in aerosols for a duration of ~ 3 hours. To obtain a better comprehension of the potential role of aerosols in virus transmission, the relationship between virus infectivity and particle size has to be carefully studied (Galton et al. 2011). Few studies are available on this topic. For example, Scott and Sydiskis 1976) reported the presence of a lower infectious dose in smaller size particles (2 µm) than in larger particles (10 µm). Thus, PM₁₀ particles can act as a more efficient carrier than PM_{2.5} particles. Furthermore, particle size may also affect virus survivability. In this regard, Tyrrell (1967) demonstrated that rhinovirus survives better in coarse particles (>4 µm) than in smaller particles (0–4 µm), while Appert et al. (2012) found that adenovirus infectivity is better preserved in coarse particles compared with fine particles.

4. Assessment of the potential role of airborne transmission

An analytical model was developed in order to better understand the potential role of airborne transmission in conveying SARS-CoV-2 in the human respiratory system through PM particles. A proper simulation of this process requires specific information on exhaled particles' sizes and concentrations, their residence time, particle collection efficiency (i.e. the combined effect of collision and coagulation efficiencies in the formation of virus-transmitting PM particles) based on a quantitative assessment of the role of Brownian diffusion, turbulent fluctuations and gravitational and drag forces, as well as transported viral dose and minimum infective dose. Only part of this information is available in the open international literature specifically for SARS-CoV-2. However, for the purpose of obtaining an approximate assessment of the role of airborne transmission, missing specific information on the above quantities for SARS-CoV-2 is replaced with analogous information from other viral pathologies. Obviously, this leads to results affected by a large degree of uncertainty. The developed analytical model assumes/considers that:

- particle pollution conditions are present, with PM concentration levels of $60 \mu\text{g}/\text{m}^3$ for both PM_{2.5} and PM₁₀ particles (this value having been overpassed on average 8 and 6 times, respectively, during the month of February 2020 in all metropolitan cities in Lombardia, see following section 1).
- SARS-CoV-2 may remain viable in aerosols for a ~ 3 hours, with a reduction in infectious titer from 10^5 to $10^{2.7}$ TCID₅₀ per liter of air (van Doremalen et al., 2020);
- small particles exhaled during breathing or speaking (with sizes typically smaller than 5 mm, 87% of which on average being smaller than 1 μm , Fairchild and Stampfer, 1987; Wan et al, 2014; Papineni et al., 1997) and coughing may colloid and coalesce with suspended PM_{2.5}/PM₁₀ particles (with sizes smaller than 2.5 and 10 mm, respectively).
- the number of particles exhaled on tidal breathing by human rhinovirus (HRV)-infected subjects was estimated to be as large as 7200 particles per liter (Fabian et al., 2011), while number of particles exhaled by mechanically ventilated patients affected by pneumonia 4644 was estimated to be as large as (Wan et al., 2014).
- 3-h pulmonary ventilation corresponds to a volume which is the tidal volume (typically ~ 500 ml, Carroll, 2007) times the respiratory rate (typically ~ 12 breaths/min, Carroll, 2007) i.e. 2160 breaths/3 h = 1080 l/3h.
- Air expelled during 3-h coughing corresponds to is the typical single coughing volume (2.5 l) times the coughing rate (typically ~ 1 cough/min).
- particles expelled during coughing in the case of influenza were estimated to be 35 % with an aerodynamic diameter larger than 4 mm in, 23 % with diameters between 1 and 4 mm and 42 % with

diameters smaller than 1 mm (Lindsley et al., 2010).

- the number of particles produced on coughing by influenza infected patients was estimated to be 29,600 particles and 16,800 after recovery (Lindsley et al., 2012).
- the velocity of particles produced on breathing was estimated to be 1-7 m s⁻¹ (Tsuda et al., 2013), while the velocity of particles produced on coughing was estimated to be 10-30 m s⁻¹ (Bourouiba, 2020).
- Particles are subject to three major classes of motion: uniform motion (primary associated with the gravitational and drag forces), diffusive motion (Brownian diffusion) and the motion of the air mass in which the particle is embedded (wind, turbulence, convective air currents,).
- As a result of gravitational settling, in combination with drag, particles reach a characteristic constant velocity v_t called *terminal settling velocity*, the characteristic time τ required for a particle to reach its terminal settling velocity varies as a function of the particle size, being 8×10^{-5} s for PM2.5 particles and 1.2×10^{-3} s for PM10 particles (Seinfeld and Pandis, 1998).
- For $t \gg \tau$, the particle attains its *terminal settling velocity* which can be determined with the following expression:

$$V_t = \frac{r_p \rho g C_c}{9\mu}$$

with r_p being the particle radius, ρ being the particle density ($1.27-1.78 \times 10^3$ kg m⁻³ for black carbon, $1.8-2.1 \times 10^3$ kg m⁻³ for soot), g being the gravity acceleration (9.8 m s⁻¹), C_c being the Slip Correction Factor (with values varying around 1 in the considered particle size range, Seinfeld and Pandis, 1998) and μ being the viscosity of air (1.8×10^{-5} kg m⁻¹s⁻¹). The above expression is applicable to motions characterized by Reynold numbers $Re < 0.1$ or particles smaller than about 20 μ m (Seinfeld and Pandis, 1998)

- PM2.5/PM10 particles have larger *terminal settling velocities* than particles exhaled while breathing, speaking and part of those emitted when coughing. As a result of this differential velocity PM2.5/PM10 particles eventually collide with exhaled particles.
- Collision efficiency associated with differential sedimentation velocities is ~ 1 because of the size difference between the colliding particles and the size of the collector droplet (PM2.5 and PM10); the collision efficiency is defined as the square of the ratio of the largest initial horizontal separation x of the falling droplet centers to the radius R of the larger droplet, i.e. $e_{coll} = (x/R)^2$ (Phan-Cong. and Dinh-Van, 1973).
- Coagulation efficiency has been studied for a variety of aerosol particles (among others, Dimmick et al., 1975). In the present study an estimate of this efficiency was obtained through an analytical model (Park et al., 1999; Otto et al., 1999) simulating the role of coagulation associated with Brownian diffusion and turbulent fluctuations, and accounting for the

differential sedimentation velocities of colliding particles, assuming liquid water to be the predominant component of exhaled particles and PM2.5/PM10 particles being assumed to be primarily carbonaceous/soot particles (density=1.8-2.1×10³ kg m⁻³), with a high affinity to water, i.e. a high hygroscopicity (Liu et al., 2013; Henning et al., 2012).

- The dynamical regime is defined through the Knudsen number of the particles:

$$K_n = \frac{2\lambda}{d}$$

where λ is the mean free path of the suspending gas and d is the diameter of the particle (Baron and Willeke, 2001). The free molecular regime characterizes particles small compared to the mean free path of the suspending gas ($Kn \gg 1$, De Carlo, 2004). In this regime, particles tend to follow ballistic streamlines. Particles in the continuum regime (Kn

$\ll 1$, De Carlo, 2004) are large compared to the mean free path of the suspending gas, with this gas acting as a continuous fluid flowing round the particle. Noting that the mean free path for air is about 0.07 μm (Jennings, 1988), the motion of the suspended particles considered in this study follows the equations governing the continuum regime.

- The collision frequency for aerosol particles in continuum regime is given the expression (Morris, 2002; Friedlander, 1977):

$$N_{ab} = \beta(a,b) \times n_a \times n_b$$

with n_a and n_b being the concentrations of the two classes of particles a and b , and $\beta(a,b)$ being the coagulation frequency in the continuum regime. The coagulation frequency can be determined through the expression (Morris, 2002):

$$\beta(a,b) = 4\pi(r_a + r_b)(D_a + D_b)$$

with $r_{a/b}$ being the radii of the two colliding particles and D_a+D_b being the effective diffusion coefficient between particles. The diffusion coefficients $D_{a/b}$ can be determined through the Stokes-Einstein relation (Seinfeld and Pandis, 1998):

$$D_{a/b} = \frac{kT C_c}{6\pi\mu r_{a/b}}$$

with k being the Boltzmann constant (1.38 J K^{-1}), C_c being the Slip Correction Factor (Seinfeld and Pandis, 1998) and μ being the viscosity of air ($1.8 \times 10^{-5} \text{ kg m}^{-1} \text{ s}^{-1}$). In air at 293 K and 1 atm, $D=1.29 \times 10^{-10}$ for 0.1- μm radius particles, $D=5.05 \times 10^{-12}$ for 1- μm radius particles, $D=4.92 \times 10^{-12}$ for 2.5- μm radius particles, $D=1.20 \times 10^{-12}$ for 10- μm radius particles.

- Based on the above analytical expressions, which describe the different microphysical processes involving PM2.5/PM10 particles and the small particles emitted during breathing, speaking or coughing, it is possible to determine the number of coalescence events associated with Brownian diffusion and turbulent fluctuations, which was estimated to be ~

5 for each PM2.5 particle and ~ 20 for each PM10 particle, while the number of coalescence events associated with the uniform vertical motion caused by gravitational and drag forces, and the consequent differential sedimentation velocities of smaller and larger particles, is estimated to be ~ 5 for each PM2.5 particle and ~ 150 for each PM10 particle. Furthermore, the overall number of coalescence events of smaller particles emitted during breathing, speaking or coughing over PM2.5/PM10 particles is estimated to be $1.4\text{-}7.0 \times 10^6$.

- The minimum infectious dose of viable SARS-CoV-2 required to cause infection is not known yet, but it was studied for other respiratory viruses. Different parameters are used to quantify this viral. One of the most frequently used is the TCID50 (Median Tissue Culture Infectious Dose), which quantifies the virus concentration needed to infect 50% of the cells of the inoculated culture (Ward et al. 1984).
- The infectious titer capable to determine a TCID50 level of infectivity was estimated for the Coronavirus to be equal to 1.6×10^6 infectious particles (Stepp et al., 2010).
- No literature information is available on the ratio of total to infectious particles for SARS-CoV-2/COVID-19. However, considering that the number of small particles coalescing on PM2.5/PM10 particles is estimated to be in the range $1.4\text{-}7.0 \times 10^6$ and the Coronavirus infectious titer was measured to be 1.6×10^6 particles, if the ratio of total to infectious particles is 5 or smaller, chances are high that airborne transmission may effectively contribute to the infectious spread.

All in all, the results from the analytical expressions representing the different microphysical processes involving suspended particles, in combination with measurements of PM2.5/PM10 particle pollution and virological and epidemiologic information and results from literature papers, allow establishing the important potential role of airborne transmission in conveying a contagious virus amount in the respiratory system, this being primarily associated with small particles emitted during breathing, speaking, and partially also during coughing, each one carrying a limited virus infective amount, which may colloid and coalesce with suspended particles, eventually leading to PM particles carrying a sufficient virus amount for the infection to be transmitted.

5. Air quality datasets

Reported PM₁₀ measurements considered in this paper for comparison with epidemiologic parameters are from the Italian ground-based network of air quality monitoring stations which is run by different Regional and Provincial Environment Agencies. Filter based samplers of PM_{2.5}/PM₁₀ particles, equipped with size-selective inlets capable to discriminate particles smaller than 2.5 and 10 μm , respectively, represent the primary approach to monitor atmospheric particulate matter in the ground network of air quality monitoring stations.

The effective impact of PM_{2.5}/PM₁₀ particles on COVID-19 infection outbreak strongly depends on particles persistency in the air, i.e. on the duration of the exposure of the human respiratory system throughout the day. However, in most cases gravimetric measurements are based on the analysis of filters collecting particulate material throughout the duration of the day, and, consequently, lack temporal resolution. Thus, ground PM measurements are scarcely usable when particle concentration variability during the day or at specific times of the day needs to be inferred. Alternative measurement techniques or datasets have then to be considered to eventually assess the actual duration of pollution exposure of the human respiratory system throughout the day. Particularly effective in this direction is the use of PM_{2.5}/PM₁₀ data from near-real-time ECMWF-CAMS analysis, which are provided with hourly resolution and grid size of 10×10 km. The CAMS near-real-time reanalysis, used in this research effort, is the most recent global reanalysis data set of atmospheric composition and air quality produced by the Copernicus Atmosphere Monitoring Service (CAMS) of the European Centre for Medium-Range Weather Forecasts (ECMWF). Particulate matter data expressed in terms of Absorbing Aerosol Index may also be inferred from the satellite sensor TROPOMI on-board Copernicus Sentinel-5P. Absorbing Aerosol Index from Sentinel-5P TROPOMI are also used in the present research effort. Sentinel-5 Precursor (5P) mission is the first Copernicus mission dedicated to monitoring our atmosphere. The mission, launched in October 2017, consists of one satellite carrying the TROPospheric Monitoring Instrument (TROPOMI) instrument. TROPOMI is a nadir-viewing, imaging spectrometer covering wavelength bands between the ultraviolet and the shortwave infrared. The satellite is located on a near-polar, sun-synchronous orbit, with high inclination (approximately 98.7°) at an altitude of approximately 824 km. The satellite performs 14 orbits per day, 227 orbits per cycle, and its orbital cycle, i.e. the time taken for the satellite to pass over the same geographical point on the ground, is 16 days. TROPOMI is a passive grating imaging spectrometer, in non-scanning nadir viewing configuration, with swath width of 2,600 km and a spatial sampling of 7×7 km². The spectrometer has 2 bands in the UV, 2 in the VIS, 2 in the NIR and 2 in the SWIR. Data from TROPOMI, with nadir overpasses at 13:30 local time (ascending node crossing time), are provided with a grid size of

3.5 × 3.5 km. TROPOMI can measure geo-located total and tropospheric columns of O₃, NO₂, SO₂, CO, HCHO and CH₄, while cloud and aerosol information are provided in terms of absorbing aerosol index and aerosol layer height. Observations of NO₂ and HCHO from TROPOMI are reported and discussed in this paper in order to assess their contribution to PM_{2.5}/PM₁₀ levels through secondary aerosol formation processes.

Results

6.1 Evolution of PM_{2.5}/PM₁₀ concentration levels throughout the month of February 2020

Figure 1 shows PM_{2.5}/PM₁₀ concentrations at 00:00 UTC on 17 February 2020, as provided by the near-real-time ECMWF-CAMS analysis. The figure covers an area extending over the latitudinal range 36-48° N and the longitudinal range 5-20° E, which encompasses the Italian peninsula together with portions of the surrounding nations. The figure clearly reveals the presence of enhanced PM_{2.5} and PM₁₀ concentration levels over large portions of the Po Valley, with levels up to 70 and 50 µg/m³, respectively, observed in Lombardy region. These values are largely exceeding the limits of 25 µg/m³ for PM_{2.5} and 50 µg/m³ for PM₁₀ defined by the WHO Air quality guideline (WHO, 2005). This figure provides a snapshot of the highly polluted conditions present in the Po Valley shortly before (1-2 weeks) the pandemic outbreak. While PM₁₀ concentrations are typically higher than PM_{2.5} concentrations, a temporary reverse situation is found in mid-late February over large portions of the Po Valley, with PM_{2.5} concentrations systematically exceeding corresponding PM₁₀ concentrations by up to 20 µg/m³. Figure 2 shows PM_{2.5}/PM₁₀ concentrations at 00:00 UTC on 29 February 2020, again from the near-real-time ECMWF-CAMS analysis. This figure provides a snapshot of pollution situation few days after the shut-down of all vehicular and industrial activities associated with the lock-down in Northern Italy on 25 February 2020. PM_{2.5}/PM₁₀ concentration levels are found to have dropped abruptly, with levels not exceeding 15-20 µg/m³ for both species.

Figure 3 illustrates the Absorbing Aerosol Index at 12:30 UTC on 17 February 2020, as inferred from the satellite sensor TROPOMI on-board the Copernicus Sentinel-5P. Data cover the same area considered in figures 1 and 2. The Absorbing Aerosol Index is a qualitative index indicating the presence of elevated aerosol layers with significant absorption. The calculation of the Absorbing Aerosol Index exploits the wavelength dependence of Rayleigh scattering in the UV spectral region. The Absorbing Aerosol Index allows to track the evolution of episodic aerosol plumes primarily from PM_{2.5}/PM₁₀ pollution, dust outbreaks and biomass burning. The figure clearly reveals the presence of a thick aerosol loading in the Po Valley, with a geographical pattern very similar to the one found in figure 1. Figure 4 illustrates the NO₂ concentration levels from TROPOMI again at 12:30 UTC on 17 February 2020 for the same area considered in figures 1-3. The figure reveals the presence of peak NO₂ values over the metropolitan area of Milan (5×10^{-4} mol m⁻²), but high values, in excess of $1.5-2 \times 10^{-4}$ mol m⁻², are observed over large portions of the Po Valley. Peak values, but of much lower amplitude ($\sim 1.5 \times 10^{-4}$ mol m⁻²), are found over the metropolitan areas of Rome and Napoli. These measurements testify the important potential

contribution of secondary aerosol formation in the observed PM_{2.5}/PM₁₀ pollution event. Figure 5 illustrates the HCHO, or formaldehyde, concentration levels from TROPOMI at the same time and over the same geographical area considered in figures 1-3. Values around 2.5×10^{-4} mol m⁻² are found in the upper portion of the Po Valley, where PM_{2.5}/PM₁₀ concentration levels are found to be higher, thus further supporting the hypothesis of the important potential role played by secondary aerosol formation. In this regard, it is to be specified that atmospheric formaldehyde is a product of isoprene oxidation (Palmer et al., 2003) and isoprene emitted by vegetation is an important precursor of secondary organic aerosols (Marais et al., 2016). Due to the low signal-to-noise ratios which characterizes Absorbing Aerosol Index and NO₂/HCHO concentration measurements, data in figure 3-5 are obtained as 7-day averages centered on the reference day, i.e. on 17 February 2020, thus including the data from 14 to 20 February 2020.

Measurements from the ground-based network of air quality monitoring stations reveal that threshold levels for PM₁₀ (<50 µg/m³) were exceeded on 20-35 days over the period January-February 2020 in many areas in the Po Valley, with levels in excess of 80 µg/m³ occasionally observed in the 1-3 weeks preceding the contagious activation around 25 February 2020. Threshold values for PM_{2.5} indicated in WHO air quality guidelines (<25 µg/m³) were exceeded on more than 40 days over the period January-February 2020 in large portions of the Po Valley, with levels up to 70 µg/m³ observed in the weeks preceding the contagious activation. More specifically, figure 6 illustrates the variability of PM_{2.5} and PM₁₀ concentration levels over the month of February 2020 for several metropolitan cities in Lombardia (Bergamo, Brescia, Cremona, Milano, Monza and Pavia) as obtained from near-real-time ECMWF-CAMS analysis. Several locations, when available, are considered for each city. The figure reveals the high PM_{2.5}/PM₁₀ peak values observed during the month of February 2020 in all considered cities, with values in excess of 60 µg/m³ observed 3 to 14 and 3 to 9 times for PM_{2.5} and PM₁₀ particles, respectively. This figure also reveals that three major particulate matter pollution outbreaks took place during the month of February 2020: a first one, covering the period 06-11 February, a second one, covering the period 15-19 February, and a third one, covering the period 20-26 February.

Figure 7 illustrates the measurements of PM_{2.5} and PM₁₀ concentration levels during the month of February 2020 from three ground-based stations, one in Bergamo (via Meucci, 45°41'24" N, 09°38'28" E) and two in Brescia (via Broletto, 45°32'23" N, 10°13'24" E; Villaggio Sereno, 45°31'04" N, 10°10'41" E) as obtained from the network of air quality monitoring stations run by different Regional and Provincial Environment Agencies. These are compared with the corresponding data from the hourly near-real-time ECMWF-CAMS analysis. ECMWF-CAMS analysis well reproduces PM_{2.5}/PM₁₀ concentration values measured by the ground-based stations, thus revealing its specific capability to capture the high resolution variability of PM_{2.5}/PM₁₀ concentration levels within each single day in this period. This comparison clearly highlights that very high peak concentration values (up to ~80 µg/m³) are occasionally observed at specific times of the day, such peaks being not detected by daily-averaged ground station measurements.

In the present research effort, for the purpose of comparing PM10 measurements with epidemiologic parameters, we focused our attention on the high PM10 pollution levels experienced over the 12 days period from 15 to 26 February 2020, when very high and persistent PM10 concentration values were observed over a major portion of the Po Valley.

6.2 Correlations between epidemiologic parameters and PM concentration levels

The effective impact of PM2.5/PM10 particles on SARS-CoV-2/COVID-19 infection outbreak is expected to be strongly dependent on particles persistency in the air, i.e. on the duration of the effective exposure to particle pollution of the human respiratory system throughout the weeks preceding the pandemic onset. In a previous paper by Borro et al. (2020) the variability of the infection rate, the mortality rate and the case fatality rate as a function of particle concentration was estimated for PM2.5 particles only, recognizing a primary role of these particles in inducing an over-expression of ACE-2 in the human respiratory system (among others, see papers by Gemmati et al., 2020; Devaux et al., 2020; Bunyavanich et al., 2020; Leung et al., 2020). In the present section we extend the analysis to PM10 particles, thus assessing the incidence of this additional pollution source on epidemiologic parameters. Specifically, PM10 concentration measurements over the period 15-26 February 2020 are compared with epidemiologic data for all 110 Italian Provinces, as reported by the Italian Statistics Institute (ISTAT, 2020), over the period 20 February- 31 March 2020. Actually, the epidemiologic data report from ISTAT includes only 107 Provinces, as in fact four Provinces in Southern Sardinia (Carbonia-Iglesias, Ogliastra, Olbia-Tempio and Medio Campidano) are grouped together as “Sud Sardegna”.

Three are the epidemiologic parameters considered in this study: the *infection rate*, or *incidence of the pathology*, quantifying the pathology appearance frequency in a particular population (Shields and Twycross, 2003), which is defined as the number of infected people in a Province normalized to the Province population; the *mortality rate* for the pathology (Gülmezoglu et al., 2004), quantifying the frequency of occurrence of death in a defined population, which is defined as the number of deaths in a Province normalized to the Province population; and the *case fatality rate* (Harrington, 2020), quantifying the proportion of deaths from a specified pathology compared to the total number of people diagnosed with the pathology, which is defined as number of reported deaths in a Province normalized to the number of reported cases.

A statistical analysis is carried out to correlate the infection rate, or incidence of the pathology, the mortality rate and the case fatality rate with PM10 concentration levels. In the previous study by Borro et al. (2020), PM2.5 pollution levels from a single station within each Province territory were considered. The present study considers PM10 concentration measurements from all ground stations available within each Province territory, which allows accounting for the natural variability of the particulate matter pollution within the single Province territories, including both urban, semi-urban and rural areas. In fact, particulate concentration variability within single Province territories is an important aspect to be properly

accounted for when correlating epidemiologic parameters with atmospheric pollution. For this purpose, particulate concentration variability within the single Province territories has been used as a weighting factor in the statistical analysis carried out to correlate epidemiologic parameters with PM10 concentration levels. Specifically, we computed the average PM10 concentration value over the period 15-26 February for each station within each Province territory. The mean and standard deviation of the average values of the different stations within each Province territory are used in the statistical analysis to be compared with the epidemiologic parameters.

Figure 8 illustrates a scatter plot comparing the mean and standard deviation values of PM10 concentration for the 110 Italian Provinces over the period 15-26 February 2020 with simultaneous mean PM2.5 concentration values. A linear fit was applied to the data points in the figure, using a linear regression function with the form $Y = A + B \times X$, with the weight given by the error bars, and obtaining the following results: $A = 8.1 \pm 0.5 \mu\text{g}/\text{m}^3$, $B = 1.04 \pm 0.02$, correlation coefficient = 0.96 and $p\text{-value} < 0.0001$. These results reveal a very high correlation between PM10 and PM2.5 concentration values in most Provinces, which testifies the simultaneous presence of both particle types in these Provinces. Specifically, based on the above reported numbers, mean PM10 concentration values are on average higher than corresponding PM2.5 values by $\sim 8 \mu\text{g}/\text{m}^3$, with the concentration growth rates being almost identical for PM2.5 and PM10 particles (4 % higher for PM10 particles with respect to PM2.5).

Coming to the results from the statistical analysis correlating epidemiologic parameters with PM10 concentration levels, the upper panel of figure 9 compares the “case fatality rate” in the period 20 February-31 March 2020 with the corresponding average PM10 concentration values in the period 15-26 February 2020 for all 110 Italian Provinces. A linear fit was applied to the data, using a linear regression function with the form $Y = A + B \times X$, with the weight given by error bars, and obtaining the following results: $A = (17.9 \pm 0.3) \mu\text{g}/\text{m}^3$, $B = (150.0 \pm 2.7) \text{m}^3/\mu\text{g}$, with the correlation coefficient being equal to 0.89. The p-value is smaller than 0.0001, which indicates less than 0.01 % probability that no statistically significant relationship is present between the two compared quantities. The slope of the regression line of the “case fatality rate” vs. PM10 concentration is $(6.7 \pm 0.3) \times 10^{-3} \text{m}^3/\mu\text{g}$, which implies a doubling (from 3 to 6 %) of the mortality rate of infected patients for an average PM10 concentration increase from 22 to 27 $\mu\text{g}/\text{m}^3$.

The middle panel of figure 9 compares the “incidence of the pathology” in the period 20 February- 31 March 2020 with the corresponding average PM10 concentration values in the period 15-26 February 2020 for the 110 Italian Provinces. The best-fit statistical analysis carried out to correlate these two parameters indicates a regression line with $A = (21.1 \pm 0.3) \mu\text{g}/\text{m}^3$ and $B = (4040 \pm 98) \text{m}^3/\mu\text{g}$, a correlation coefficient equal to 0.82 and $p\text{-value} < 0.0001$. The slope of the regression line of the “incidence of the pathology” vs. PM10 concentration is $(2.48 \pm 0.6) \times 10^{-4} \text{m}^3/\mu\text{g}$, which implies a doubling (from 1 to 2 ‰) of the incidence of the pathology for an average PM10 concentration increase from 25 to 29 $\mu\text{g}/\text{m}^3$.

The lower panel of figure 9 compares illustrates the “mortality rate” in the period 20 February-31 March 2020 with the corresponding average PM10 concentration values in the period 15-26 February 2020 for the 110 Italian Provinces. The linear regression analysis leads the following results: $A = (23.9 \pm 0.3) \mu\text{g}/\text{m}^3$

and $B = (18312 \pm 454) \text{ m}^3/\mu\text{g}$, a correlation coefficient equal to 0.80 and $p\text{-value} < 0.0001$. The slope of the regression line of the “mortality rate” vs. PM10 concentration is $(5.46 \pm 0.14) \times 10^{-5} \text{ m}^3/\mu\text{g}$, which implies a tripling (from 0.1 to 0.3 ‰) of the mortality rate for an average PM10 concentration increase from 25 to 29 $\mu\text{g}/\text{m}^3$.

It is to be specified that results illustrated in the present paper reveal the presence of much higher correlation coefficients between the epidemiologic parameters and PM10 concentration levels than those reported in the paper by Borro et al. (2020) (0.89 against 0.7 for the “case fatality rate” versus PM concentration levels, 0.80 against 0.65 for the mortality rate versus PM concentration levels and

0.82 against 0.67 for the incidence of the pathology versus PM concentration levels). The higher values found in the present correlation analyses between epidemiologic parameters and PM concentration levels are to be attributed to several motivations. First, the present correlation analyses are considering PM10 particles instead of PM2.5 particles. Secondly, the present analyses are considering PM concentration levels, properly accounting for their variability within the single Province territories, using this variability as a weighting factor in the regression analysis. This implies that, in the best fit analysis, data points characterized by a higher variability of PM concentration levels are considered with a lower weight. This approach is certainly very effective in properly filtering potential biases associated with the use of a single pollution monitoring station in each Province territory, especially in those cases when PM pollution levels sensitively vary within the Province territory. Correlation coefficient values in the range 0.80-0.89 testify a high statistical significance. In this regard, it is to be underlined that the correlation coefficient quantifies the strength and direction of the linear relationship between two variable quantities, with the reliability of the linear model depending on the number observed data points. Thus, both the correlation coefficient value and the number data points need to be properly accounted for in the assessment of the significance of the results. In general, the larger is the number data points, the lower is the acceptable correlation coefficient.

It is also to be underlined that correlation results between the different epidemiologic parameters and PM concentration levels are strongly dependent on the considered elapsed time lag between the pollution events and the time interval considered for the assessment of the epidemiologic parameters, as well as on the duration of the considered pollution time window. In general, the consideration of a possible time gap between population exposure to enhanced PM concentration levels and the onset of the infection, and the eventual death of patients, ensures that the pollution exposition period is long enough to induce a biological response in human tissues. A sensitivity study was carried out considering different time gaps and pollution integration times. In the sensitivity analysis there was no possibility to also vary the time window considered for the epidemiologic parameters as in fact these were provided by the Italian Statistics Institute uniquely for the period 20 February-31 March 2020 (ISTAT, 2020). Specifically, we considered three different time windows for particle pollution: 01-26 February 2020, 01-19 February 2020 and 15-26 February 2020. The first time window allows including all three major pollution outbreaks in February 2020 identified in figure 6, i.e. 06-11 February, 15-19 February and 20-26 February. The second time window includes the first two pollution outbreak events, while the third time window includes the last

two pollution outbreak events. Results reveal a maximum correlation when comparing the epidemiologic parameters in the period 20 February-31 March 2020 versus the corresponding average PM concentration values observed in the period 15-26 February 2020 (for example, the statistical analysis correlating the “case fatality rate” to PM concentration levels leads to a correlation coefficient equal to 0.89 when considering PM10 concentration measurements over the period 15-26 February 2020, equal to 0.72 when considering PM10 concentration measurements over the period 01-26 February 2020 and 0.70 when considering PM10 concentration measurements over the period 01-19 February 2020).

The revealed positive correlation between epidemiologic factors and PM10 concentration levels identified in this paper does not imply a direct and univocal cause-effect relation, but PM pollution is certainly one of the several factors that influenced the pandemic outbreak in Northern Italy in the period February-March 2020. In principle, some other circumstance could have caused both epidemiologic factors and PM10 concentration levels to change.

We also investigated the role of population density, which was quantified to be far less important than PM pollution. Figure 9 shows the linear regression analysis correlating population density with the incidence of the pathology (upper panel), the mortality rate (middle panel) and the case fatality rate (lower panel) in the period 20 February-31 March 2020. This analysis is again extended over all 110 Italian Provinces. Specifically, the statistical analysis correlating the incidence of the pathology with population density reveals a totally missing correlation, with a correlation coefficient of 0.045 (figure 9, upper panel). The p-value is equal to 0.65, which indicates 65 % probability that no statistically significant relationship is present between the two compared quantities. The statistical analysis correlating the mortality rate with population density reveals a very low correlation, with a correlation coefficient of 0.19 and a p-value equal to 0.051 (figure 9, middle panel). Finally, the correlating the case fatality rate with population density reveals an almost totally missing correlation, with a correlation coefficient of 0.093 and a p-value equal to 0.34 (figure 9, lower panel).

The reported statistical results do not completely exclude a correlation between the above mentioned epidemiologic parameters and population density: they only underline that there are so many outliers in the analysis to make this correlation meaningless. More specifically, the different panels of figure 9 reveal the presence of data points with very scattered distributions. These distributions imply that outliers are present in the analysis, i.e. there is a certain number of provinces with low population density and high values of the epidemiologic parameters and a certain number of provinces with high population density and low values of the epidemiologic parameters, these data points severely compromising the regression analysis. For example, Provinces as Napoli, Monza and Trieste are characterized by quite high population densities, but have low values of the epidemiologic parameters and were only poorly affected by COVID-19. Analogously, Provinces as Cremona, Lodi and Piacenza are characterized by low population densities, but were severely affected by COVID-19. Obviously, few outliers were also present in the statistical analysis correlating the epidemiologic parameters with PM10 concentration levels (for example, the Province of Aosta in Valle d’Aosta, where a large number of hospitalizations refer to patients coming from other areas of the Italian territory as a result of their short-term mobility associated with winter skiing

holidays). However, these outliers were very few and their presence only slightly affected the results of the regression analysis.

Conclusions

Summary and final remarks

The devastating impact in terms of number of infected people and deaths associated with the COVID-19 pandemic in the early portion of 2020 was the result of a variety of contributory causes and circumstances. While the spread and effective impact of the SARS-CoV-2 virus was primarily related to the life styles and social habits of the different human communities and the presence of specific hotbeds generated by infected people returning from travels abroad, environmental and meteorological factors have possibly also played a role.

In the present paper we have illustrated the evolution of PM_{2.5}/PM₁₀ concentration levels throughout the month of February 2020, identifying in the central part of the month the presence of enhanced PM_{2.5} and PM₁₀ concentration levels over large portions of the Po Valley, with levels up to 70 and 50 $\mu\text{g}/\text{m}^3$, respectively, observed in Lombardy region. A marked reduction of pollution levels was observed in the part of the month, few days after the shut-down of all vehicular and industrial activities associated with the lock-down in Northern Italy on 25 February 2020, with PM_{2.5}/PM₁₀ concentration levels abruptly dropped to levels not exceeding 15-20 $\mu\text{g}/\text{m}^3$ for both species.

A simulation based on the use of an analytical microphysical model capable to simulate the different coagulation processes (Brownian diffusion, turbulent fluctuations and gravitational and drag forces) taking place in the formation of virus-transmitting PM particles, in combination with PM_{2.5}/PM₁₀ pollution measurements and specific literature information on exhaled particles' sizes and concentrations, their residence time, transported viral dose and minimum infective dose, allowed getting a preliminary assessment of the potential role of airborne transmission through virus-transmitting PM particles in conveying SARS-CoV-2 in the human respiratory system.

In the paper we have also reported results from a statistical analysis correlating the infection rate, or incidence of the pathology, the mortality rate and the case fatality rate with PM concentration levels, which reveals a high correlation of these epidemiologic parameters with PM₁₀ concentration levels (correlation coefficients in the range 0.80-0.89), with the case fatality rate doubling (from 3 to 6 %) for an average PM₁₀ concentration increase from 22 to 27 $\mu\text{g}/\text{m}^3$ and the infection rate doubling (from 1 to 2 ‰) and the mortality rate a tripling (from 0.1 to 0.3 ‰) for average PM₁₀ concentration increase from 25 to 29 $\mu\text{g}/\text{m}^3$.

Correlations between epidemiologic factors and PM concentration levels do not imply a relation of cause-effect between the onset of the pandemic and PM pollution. The reported correlation has to be interpreted in a mathematical sense, that is it testifies a co-occurrence of low/high values of COVID-19

epidemiologic parameters and low/high pollution levels. In the interpretation of the meaning of the high correlation coefficient values obtained in the present study, the possible occurrence of spurious correlations due to indirect causes or remote mechanisms has to be carefully accounted for (among others, Bolton, 1994). Nevertheless, results from this paper clearly testify that PM pollution is one of the several factors, certainly an important one, which affects COVID-19 incidence. A more quantitative assessment of the contributing role of PM pollution on early 2020 COVID-19 outbreak in Northern Italy implies further dedicated studies, possibly using additional experimental data, with statistics representing one of the several needed tools to be used in the investigation. The experimental/modelling evidence reported in this paper certainly calls for additional studies, possibly focusing on the quantitative assessment of all possible contributing causes based on dedicated sensitivity analyses.

Declarations

Acknowledgments

I wish to strongly acknowledge Dr. Stefano Natali and MEEO S.r.l. for the provision of ECMWF- CAMS analysis data and its graphical display through the ADAM platform (<https://adamplatform.eu>).

Conflict of interest statement

On behalf of all authors, the corresponding author states that there is no conflict of interest.

References

- Alford RH, Kasel JA, Gerone PJ, Knight V. Human influenza resulting from aerosol inhalation. *Proceedings of the Society for Experimental Biology and Medicine*. 1966;122:800–804.
- Allen, A.G., Nemitz E., Shi J. P., Harrison R. M., Greenwood J. C. Size distributions of trace metals in atmospheric aerosols in the United Kingdom. *Atmos. Environ.*, 35, 4581–4591, 2001.
- Appert, J., Raynor, P. C., Abin, M., Chander, Y., Guarino, H., Goyal, S. M., et al. (2012). Influence of Suspending Liquid, Impactor Type, and Substrate on Size-Selective Sampling of MS2 and Adenovirus Aerosols. *Aerosol Sci. Technol.*, 46:249–257.
- ARPA Lombardia, *Relazione di Monitoraggio Triennale del Piano Regionale degli Interventi per la qualità dell'aria (PRIA)*, 2017.
- Asadi S, Bouvier N, Wexler AS, Ristenpart WD. The coronavirus pandemic and aerosols: Does COVID-19 transmit via expiratory particles? *Aerosol Sci Technol*. 2020;54:635-8.
- Baron, P. A. & Willeke, K. (2001). "Gas and Particle Motion". *Aerosol Measurement: Principles, Techniques, and Applications*.

Best, E. L.; Sandoe, J. A. T.; Wilcox, M. H. (2012). "Potential for aerosolization of *Clostridium difficile* after flushing toilets: The role of toilet lids in reducing environmental contamination risk". *Journal of Hospital Infection*. 80 (1): 1–5. doi:10.1016/j.jhin.2011.08.010. PMID 22137761.

Bolton, S., *Pharmaceutical Statistics, Practical and Clinical Applications*, 3rd ed. (New York: Marcel Dekker, 1994), 252.

Borro, M., P. Di Girolamo, G. Gentile, O. De Luca, R. Preissner, A. Marcolongo, S. Ferracuti and M. Simmaco, Evidence-based Considerations Exploring Relations between SARS-CoV-2 Pandemic and Air Pollution: Involvement of PM2.5-mediated Up-regulation of the Viral Receptor ACE-2, *International Journal of Environmental Research and Public Health*, 17, 5573, doi:10.3390/ijerph17155573, 2020.

Bourouiba L. Turbulent Gas Clouds and Respiratory Pathogen Emissions: Potential Implications for Reducing Transmission of COVID-19. *JAMA*. 2020;323(18):1837-1838.

Brunekreef, B. (1997) Air pollution and life expectancy: is there a relation? *Journal of Occupational and Environmental Medicine* 54, 781-784.

Bunyavanich, S., Do A., Vicencio A. Nasal Gene Expression of Angiotensin-Converting Enzyme 2 in Children and Adults. *JAMA*. 2020;323(23):2427–2429. doi:10.1001/jama.2020.8707.

Cai J, Sun W, Huang J, Gamber M, Wu J, He G. Indirect virus transmission in cluster of COVID-19 cases, Wenzhou, China, 2020. *Emerg Infect Dis*. 2020 Jun [date cited]. <https://doi.org/10.3201/eid2606.200412>.

Carroll, R. G., 10 - Pulmonary System, Editor(s): Robert G. Carroll, Elsevier's Integrated Physiology, Mosby, pages 99-115, ISBN 9780323043182, <https://doi.org/10.1016/B978-0-323-04318-2.50016-9>, 2007.

Couch RB, Cate TR, Douglas RG, Jr, Gerone PJ, Knight V. Effect of route of inoculation on experimental respiratory viral disease in volunteers and evidence for airborne transmission. *Bacteriological Reviews*. 1966;30:517–529.

Cui, Y.; Zhang, Z.-F.; Froines, J.R.; Zhao, J.; Wang, H.; Yu, S.-Z.; Detels, R. Air pollution and case fatality of SARS in the People's Republic of China: An ecologic study. *Environ. Health* 2003, 2, 15.

De Carlo, P.F. (2004). "Particle Morphology and Density Characterization by Combined Mobility and Aerodynamic Diameter Measurements. Part 1: Theory". *Aerosol Science & Technology*. 38 (12): 1185–1205.

Devaux CA, Rolain JM, Raoult D. ACE2 receptor polymorphism: Susceptibility to SARS-CoV-2, hypertension, multi-organ failure, and COVID-19 disease outcome. *J Microbiol Immunol Infect*. 2020;53(3):425-435.

- Dimmick, R.L., A. Boyd, H. Wolochow, A simple method for estimation of coagulation efficiency in mixed aerosols, *Journal of Aerosol Science*, Volume 6, Issue 5, Pages 375-377, ISSN 0021-8502, [https://doi.org/10.1016/0021-8502\(75\)90025-7](https://doi.org/10.1016/0021-8502(75)90025-7), 1975.
- Dockery DW, Pope CA, Xu X, Spengler JD, Ware JH, Fay ME, Ferris BG, Speizer FE (1993) An association between air pollution and mortality in six U.S. cities. *New England Journal of Medicine* 329, 1753-1759.
- Fabian, P., McDevitt, J. J., DeHaan, W. H., Fung, R. O. P., Cowling, B. J., Chan, K. H., et al. (2008). Influenza Virus in Human Exhaled Breath: An Observational Study. *PloS one*, 3:e2691. DOI: 10.1371/journal.pone.0002691.
- Fabian P, Brain J, Houseman EA, Gern J, Milton DK. Origin of exhaled breath particles from healthy and human rhinovirus-infected subjects. *J Aerosol Med Pulm Drug Deliv.* 2011;24(3):137- 147. doi:10.1089/jamp.2010.0815
- Fairchild CI, Stampfer JF (1987) Particle concentration in exhaled breath. . *Am Ind Hyg Assoc J.* 48(11): 948–949.
- Friedlander S K. *Smoke, Dust and Haze – Fundamentals of Aerosol Behavior*. New York: Wiley-Interscience, 1977.
- Gemmati D, Bramanti B, Serino ML, Secchiero P, Zauli G, Tisato V. COVID-19 and Individual Genetic Susceptibility/Receptivity: Role of ACE1/ACE2 Genes, Immunity, Inflammation and Coagulation. Might the Double X-chromosome in Females Be Protective against SARS-CoV-2 Compared to the Single X-Chromosome in Males? *Int J Mol Sci.* 2020;21(10):E3474.
- Gralton, J., Tovey E., McLaws M. L., Rawlinson W. D. The role of particle size in aerosolised pathogen transmission: a review. *J Infect.* 2011;62(1):1-13. doi:10.1016/j.jinf.2010.11.010.
- Gralton J, Tovey ER, McLaws ML, Rawlinson WD. Respiratory virus RNA is detectable in airborne and droplet particles. *J Med Virol.* 2013;85(12):2151-2159. doi:10.1002/jmv.23698.
- Gülmezoglu AM, Say L, Betrán AP, Villar J, Piaggio G. WHO systematic review of maternal mortality and morbidity: methodological issues and challenges, *BMC Med Res Methodol.*, 05;4:16, 2004.
- Harrington RA. Case fatality rate. *Encyclopædia Britannica website.* <https://www.britannica.com/science/case-fatality-rate>. Last Accessed June 12th, 2020.
- Harrison RM, Tilling R, Callen Romero MS, Harrad S, Jarvis K. A study of trace metals and polycyclic aromatic hydrocarbons in the roadside environment. *Atmos. Environ.*, 37:2391–2402, 2003.
- Hemmes, J. H., Winkler, K. C., and Kool, S. M. (1960). Virus Survival as a Seasonal Factor in Influenza and Poliomyelitis. *Nature*, 188:430–431.

Henning, S., Ziese, M., Kiselev, A., Saathoff, H., Möhler, O., Mentel, T. F., Buchholz, A., Spindler, C., Michaud, V., Monier, M., Sellegri, K., and Stratmann, F.: Hygroscopic growth and droplet activation of soot particles: uncoated, succinic or sulfuric acid coated, *Atmos. Chem. Phys.*, 12, 4525–4537, <https://doi.org/10.5194/acp-12-4525-2012>, 2012.

Hodan, William M. and William R. Barnard (2004). "Evaluating the Contribution of PM 2.5 Precursor Gases and Re-entrained Road Emissions to Mobile Source PM 2.5 Particulate Matter Emissions." *Environmental Science*, ID: 28139041.

Hoek B, Brunekreef G, Goldbohm S, Fischer P, van den Brandt PA (2002) Association between mortality and indicators of traffic-related air pollution in the Netherlands: a cohort study, *The Lancet* 360, 1203-1209.

Ijaz, M. K., Brunner, A. H., Sattar, S. A, Nair, R. C., and Johnson-Lussenburg, C. M. (1985). Survival Characteristics of Airborne Human Coronavirus 229E. *J. Gen. Virol.*, 66:2743–2748.

Ijaz, M. K., Karim, Y. G., Sattar, S. A., and Johnson-Lussenburg, C. M. (1987). Development of Methods to Study the Survival of Airborne Viruses. *J. Virol. Methods*, 18:87–106.

Kim S. W., M. A. Ramakrishnan, P. C. Raynor, S. M. Goyal. Effects of humidity and other factors on the generation and sampling of a coronavirus aerosol. *Aerobiologia (Bologna)*. 2007;23(4):239- 248. doi:10.1007/s10453-007-9068-9.

Kim, J. M., Chung, Y. S., Jo, H. J., Lee, N. J., Kim, M. S., Woo, S. H., Park, S., Kim, J. W., Kim, H. M., & Han, M. G. (2020). Identification of Coronavirus Isolated from a Patient in Korea with COVID-19. *Osong public health and research perspectives*, 11(1), 3–7. <https://doi.org/10.24171/j.phrp.2020.11.1.02>.

Kumar, S. and Sunder Raman, R.: Inorganic ions in ambient fine particles over a National Park in central India: Seasonality, dependencies between SO₂, NO₃, and NH₄, and neutralization of aerosol acidity, *Atmos. Environ.*, 143, 152–163, 2016.

Jennings, S.G., The mean free path in air, *Journal of Aerosol Science*, Volume 19, Issue 2, 1988, Pages 159-166, ISSN 0021-8502, [https://doi.org/10.1016/0021-8502\(88\)90219-4](https://doi.org/10.1016/0021-8502(88)90219-4).

Jeong-Min Kim, Yoon-Seok Chung, Hye Jun Jo, Nam-Joo Lee, Mi Seon Kim, Sang Hee Woo, Sehee Park, Jee Woong Kim, Heui Man Kim, Myung-Guk Han, Identification of Coronavirus Isolated from a Patient in Korea with COVID-19, *Osong Public Health Res Perspect*. 11(1):3-7 doi: 10.24171/j.phrp.2020.11.1.02, 2020.

Jia G, Jia J (2014) Atmospheric Residence Times of the Fine-aerosol in the Region of South Italy Estimated from the Activity Concentration Ratios of ²¹⁰Po/²¹⁰Pb in Air Particulates. *J Anal Bioanal Tech* 5: 216 doi:10.4172/2155-9872.1000216.

Johnson, G. R.; Morawska, L. (2009). "The Mechanism of Breath Aerosol Formation". *Journal of Aerosol Medicine and Pulmonary Drug Delivery*. 22 (3): 229–237. CiteSeerX 10.1.1.651.7875. doi:10.1089/jamp.2008.0720. PMID 19415984.

Lakdawala, S., and Gaglia, M., What We Do and Do Not Know About COVID-19's Infectious Dose and Viral Load, *The Conversation*, April 18, 2020, <https://theconversation.com/what-we-do-and-do-not-know-about-covid-19s-infectious-dose-and-viral-load-135991>.

Lau LLH, Cowling BJ, Fang VJ, Chan KH, Lau EHY, Lipsitch M, Cheng CKY, Houck PM, Uyeki TM, Peiris JSM, Leung GM. 2010. Viral shedding and clinical illness in naturally acquired influenza virus infections. *J Infect Dis* 201:1509–1516.

Leung, J. M., Yang C. X., Tam A., et al. ACE-2 expression in the small airway epithelia of smokers and COPD patients: implications for COVID-19. *Eur Respir J*. 2020;55(5):2000688.

Li T, Zhang Y, Wang J, Xu D, Yin Z, Chen H, et al. All-cause mortality risk associated with long-term exposure to ambient PM_{2.5} in China: a cohort study. *Lancet Public Health*. 2018;3(10):e470- e477.

Lindsley WG, Blanchere FM, Thewlis RE, Vishnu A, Davis KA, Cao G, Palmer JE, Clark KE, Fisher MA, Khakoo R, Beezhold DH. 2010. Measurements of airborne influenza virus in aerosol particles from human coughs. *PLoS ONE* 5:e15100.

Lindsley WG, Pearce TA, Hudnall JB, Davis KA, Davis SM, Fisher MA, Khakoo R, Palmer JE, Clark KE, Celik I, Coffey CC, Blachere FM, Beezhold DH. 2012. Quantity and size distribution of cough-generated aerosol particles produced by influenza patients during and after illness. *J Occup Environ Hyg* 9:443–449.

Liu, D., Allan, J., Whitehead, J., Young, D., Flynn, M., Coe, H., McFiggans, G., Fleming, Z. L., and Bandy, B.: Ambient black carbon particle hygroscopic properties controlled by mixing state and composition, *Atmos. Chem. Phys.*, 13, 2015–2029, <https://doi.org/10.5194/acp-13-2015-2013>, 2013.

Liu Y, Ning Z, Chen Y, Aerodynamic analysis of SARS-CoV-2 in two Wuhan hospitals, *Nature*. 2020; 582: 557-560.

Losacco C, Perillo A. Particulate Matter Air Pollution and Respiratory Impact on Humans and Animals. *Environ Sci Pollut Res Int*. 2018;25(34):33901-33910.

Marais, E. A., Jacob, D. J., Jimenez, J. L., Campuzano-Jost, P., Day, D. A., Hu, W., Krechmer, J.,

Zhu, L., Kim, P. S., Miller, C. C., Fisher, J. A., Travis, K., Yu, K., Hanisco, T. F., Wolfe, G. M., Arkinson, H. L., Pye, H. O. T., Froyd, K. D., Liao, J., and McNeill, V. F.: Aqueous-phase mechanism for secondary organic aerosol formation from isoprene: application to the southeast United States and co-benefit of SO₂ emission controls, *Atmos. Chem. Phys.*, 16, 1603–1618, <https://doi.org/10.5194/acp-16-1603-2016>, 2016.

Mittal R, Ni R, Seo J-H. The flow physics of COVID-19. *J Fluid Mech.* 2020;894.

Morawska L, Johnson G, Ristovski Z, Hargreaves M, Mengersen KL, et al. (2009) Size distribution and sites of origin of droplets expelled during expiratory activities. . *J Aerosol Sci.* 40(3): 256–269.

Morawska L, Cao J. Airborne transmission of SARS-CoV-2: The world should face the reality. *Environ Int.* 2020;139:105730.

Morris, J. W., *Chemical Kinetics and Microphysics of Atmospheric Aerosols*, doctoral thesis, 2002.

Nicas M, Nazaroff WW, Hubbard A. Toward understanding the risk of secondary airborne infection: emission of respirable pathogens. *J Occup Environ Hyg.* 2005;2(3):143-154.
doi:10.1080/15459620590918466.

Otto, E., H. Fissan, S. H. Parkt and K. W. Leet. The log-normal size distribution theory of Brownian aerosol coagulation for the entire particle size range: Part I - analytical solution using Dahneke's Coagulation Kernel *J. Aerosol Sci.* Vol. 30, No. 1, pp. 17-34, 1999.

Pandolfi M, Gonzalez-Castanedo Y, Alastuey A, de la Rosa J, Mantilla E, Sanchez de la Campa A, Querol X, Pey J, Amato F, Moreno T. Source apportionment of PM10 and PM2.5 at multiple sites in the strait of Gibraltar by PMF: impact of shipping emissions. *Environ Sci Pollut Res*,18:260–9, 2011.

Papineni, R.S., Rosenthal, F.S. (1997) The size distribution of droplets in the exhaled breath of healthy human subjects. . *J Aerosol Med.* 10(2): 105–116.

Park, S. H., Lee, K. W., Otto, E. and Fissan, H. (1999) The log-normal size distribution theory of Brownian aerosol coagulation for the entire particle size range: Part I. Analytical solution using the harmonic mean coagulation kernel. *J. Aerosol Sci.* 30, 3-16.

Phan-Cong, L. and Dinh-Van, P. (1973) Direct measurements of coalescence efficiency and frequency of small water droplets in an electric field, *Tellus*, 25:1, 63-68, DOI: 10.3402/tellusa.v25i1.9645

Pnueli D., C. Gutfinger & M. Fichman: A Turbulent-Brownian Model for Aerosol Coagulation, *Aerosol Science and Technology*, 14:2, 201-209, DOI: 10.1080/02786829108959483, 1991.

Pope CA, Thun MJ, Namboodiri MM, Dockery DW, Evans JS, Speizer FE, Heath CW (1995) Particulate air pollution as a predictor of mortality in a prospective study of U.S. adults. *American Journal of Respiratory and Critical Care Medicine* 151, 669-674.

Pruppacher and Klett, *Microphysics of Clouds and Precipitation*, (Kluwer, 1997, 454).

Pyankov O. V., Bodnev, S. A., Pyankova, O. G., Agranovski, I. E. Survival of aerosolized coronavirus in the ambient air. *J Aerosol Sci.* 2018;115:158–63

- Ram, K. and Sarin, M. M.: Day-night variability of EC, OC, WSOC and inorganic ions in urban environment of Indo-Gangetic Plain: Implications to secondary aerosol formation, *Atmos. Environ.*, 45, 460–468, <https://doi.org/10.1016/j.atmosenv.2010.09.055>, 2011.
- Rastogi, N., Singh, A., Sarin, M. M., and Singh, D.: Temporal variability of primary and secondary aerosols over northern India: Impact of biomass burning emissions, *Atmos. Environ.*, 125, 396–403, <https://doi.org/10.1016/j.atmosenv.2015.06.010>, 2016.
- Samara C, Kouimtzis Th, Tsitouridou R, Kanias G, Simeonov V. Chemical mass balance source apportionment of PM₁₀ in an industrialized urban area of Northern Greece. *Atmos. Environ.*, 37:41–54, 2003.
- Santarpia JL, Rivera DN, Herrera V, Aerosol and surface transmission potential of SARS-CoV-2, *medRxiv*. 2020; (<https://doi.org/2020.03.23.20039446> published online June 3).
- Sattar, S. A., and Ijaz, M. K. (1987). Spread of viral infections by aerosols. *Critical Reviews in Environmental Control*, 17(2). <https://doi.org/10.1080/10643388709388331>.
- Schaffer F.L., Soergel M.E., Straube D.C., Survival of airborne influenza virus: effects of propagating host, relative humidity, and composition of spray fluids. *Arch Virol*. 1976; 51: 263- 273.
- Scott, G. H., and Sydiskis, R. J. (1976). Responses of Mice Immunized with Influenza Virus by Aerosol and Parenteral Routes. *Infect. Immunity*, 13:696–703
- Seinfeld J.H., Pandis S.N., 1998, *Atmospheric Chemistry and Physics: From Air Pollution to Climate Change*. Wiley, NY, USA, pp. 408–442.
- Setti, L., F. Passarini, G. De Gennaro, P. Barbieri, M. G. Perrone, M. Borelli, J. Palmisani³, A. Di Gilio, V. Torboli, A. Pallavicini, M. Ruscio, P. Piscitelli, A. Miani, SARS-Cov-2 RNA Found on Particulate Matter of Bergamo in Northern Italy: First Preliminary Evidence, *Environmental Research* doi: 10.1016/j.envres.2020.109754, 2020.
- Shields L, Twycross A. The difference between incidence and prevalence, *Nursing Children and Young People*, 15, 7, 50-50, doi: 10.7748/paed.15.7.50.s31, 2003.
- Smoluchowski, M. (1916). Zusammenfassende Bearbeitungen. Drei Vorträge über Diffusion, Brownsche Molekularbewegung und Koagulation von Kolloidteilchen. *Phys. Z.* 17:557.
- Smoluchowski, M. (1918). Versuch einer mathematischen Theorie der Koagulationskinetik kolloider Lösungen. *A. Phys. Chem.* 92:129.
- Stepp, P. C., Ranno, K. A., Ferris, M. M., 2010. New method for rapid virus quantification. *Genet. Eng. Biotechnol. News* 30(24).

Taiwo, A. M., D. C.S. Beddows, Z. Shi, R. M. Harrison, Mass and number size distributions of particulate matter components: Comparison of an industrial site and an urban background site, *Science of The Total Environment*, Volume 475, 2014, Pages 29-38, ISSN 0048-9697, <https://doi.org/10.1016/j.scitotenv.2013.12.076>.

Tang, J. W.; Settles, G. S. (2008). "Coughing and Aerosols". *New England Journal of Medicine*. 359 (15): e19. doi:10.1056/NEJMicm072576. PMID 18843121.

Tellier, R. (2009). Aerosol transmission of influenza A virus: a review of new studies *J. R. Soc. Interface*. 6S783–S790, <http://doi.org/10.1098/rsif.2009.0302.focus>.

Tsuda, A., Henry, F. S., & Butler, J. P. (2013). Particle transport and deposition: basic physics of particle kinetics. *Comprehensive Physiology*, 3(4), 1437–1471. <https://doi.org/10.1002/cphy.c100085>

Tyrrell, D. A. J. (1967). The Spread of Viruses of the Respiratory Tract by the Airborne Route, *Symp. Soc. Gen. Microbiol.*, 17:286–306.

van Doremalen et al., Aerosol and Surface Stability of SARS-CoV-2 as Compared with SARS- CoV-1, *The New England Journal of Medicine*, 2020.

Vecchi, R., Marcazzan, G.M., Valli, G., 2005. Seasonal variation of 210Pb activity concentration in outdoor air of Milan (Italy). *Journal of Environmental Radioactivity* 82, 251–286.

Vecchi, R., G. Marcazzan, G. Valli, A study on nighttime–daytime PM10 concentration and elemental composition in relation to atmospheric dispersion in the urban area of Milan (Italy) *Atmospheric Environment* 41 2136–2144 (2007).

Verrilli, S. et al., PM2.5 Size Distribution and Characterization by Carbon Isotope in Tuscany (Italy), *Advanced Atmospheric Aerosol Symposium*, 19-22 September 2010 Florence, Italy.

Xie X, Li Y, Chwang AT, Ho PL, Seto WH. How far droplets can move in indoor environments– revisiting the Wells evaporationfalling curve. *Indoor Air* 2007; **17**: 211–25.

Yezli, Saber, and Jonathan A. Otter. "Minimum Infective Dose of the Major Human Respiratory and Enteric Viruses Transmitted Through Food and the Environment." *Food and Environmental Virology* vol. 3,1 (2011): 1–30. doi:10.1007/s12560-011-9056-7.

Wan, G. H., Wu, C. L., Chen, Y. F., Huang, S. H., Wang, Y. L., & Chen, C. W. (2014). Particle size concentration distribution and influences on exhaled breath particles in mechanically ventilated patients. *PloS one*, 9(1), e87088. <https://doi.org/10.1371/journal.pone.0087088>.

WHO. Air quality guidelines for particulate matter, ozone, nitrogen dioxide and sulfur dioxide. Global update 2005,

https://apps.who.int/iris/bitstream/handle/10665/69477/WHO_SDE_PHE_OEH_06.02_eng.pdf?sequence=1. Last Accessed July 12th, 2020.

WHO. Modes of transmission of virus causing COVID-19: implications for infection prevention and control (IPC) precaution recommendations, Scientific Brief, 29 March 2020, 2020a.

WHO. Transmission of SARS-CoV-2: implications for infection prevention precautions, Scientific Brief, 9 July 2020, 2020b.

Zady, M. F., Correlation and simple least squares regression (October 2000).
<http://www.westgard.com/lesson44.htm>.

Figures

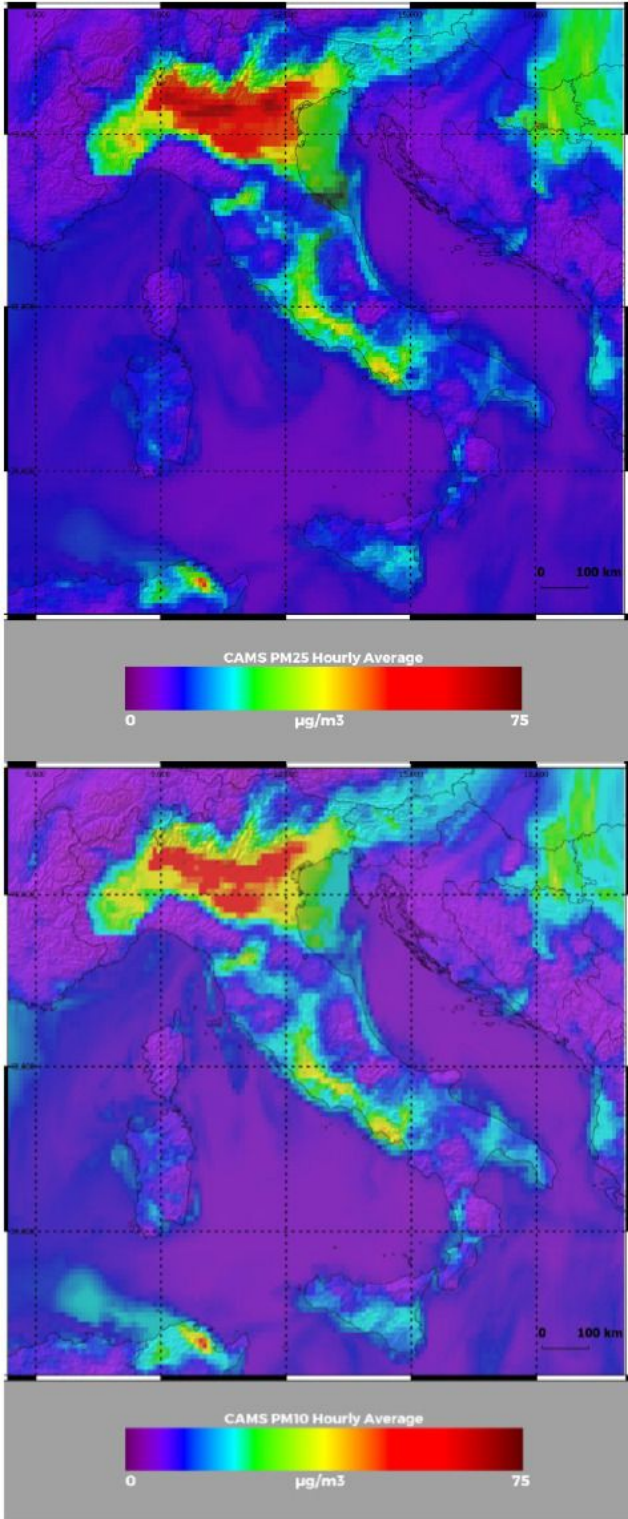


Figure 1

PM2.5 (upper panel) and PM10 (lower panel) concentration levels at 00:00 UTC on 17 February 2020 from near-real-time ECMWF-CAMS analysis over an area extending over the latitudinal interval 36-48° N and the longitudinal interval 5-20° E.

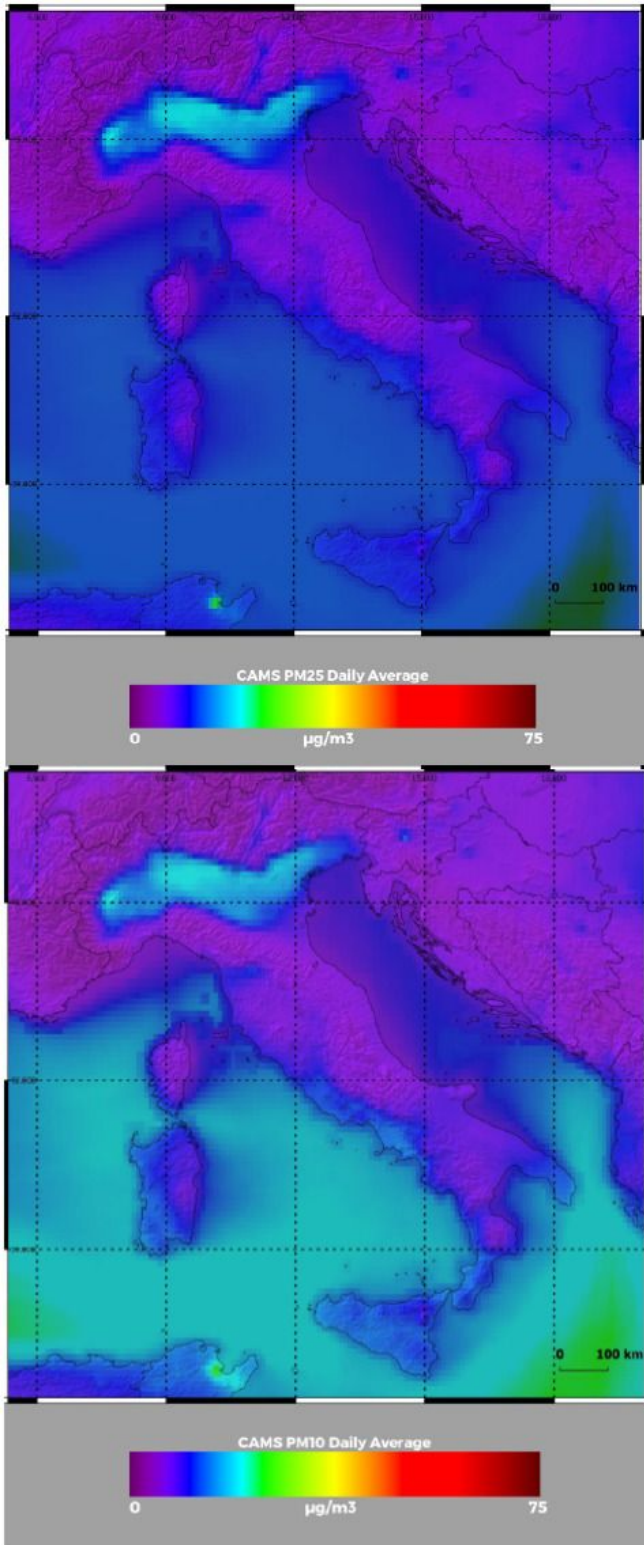


Figure 2

PM2.5 (upper panel) and PM10 (lower panel) concentration levels at 00:00 UTC on 29 February 2020 from near-real-time ECMWF-CAMS analysis over an area extending over the latitudinal interval 36-48° N and the longitudinal interval 5-20° E.

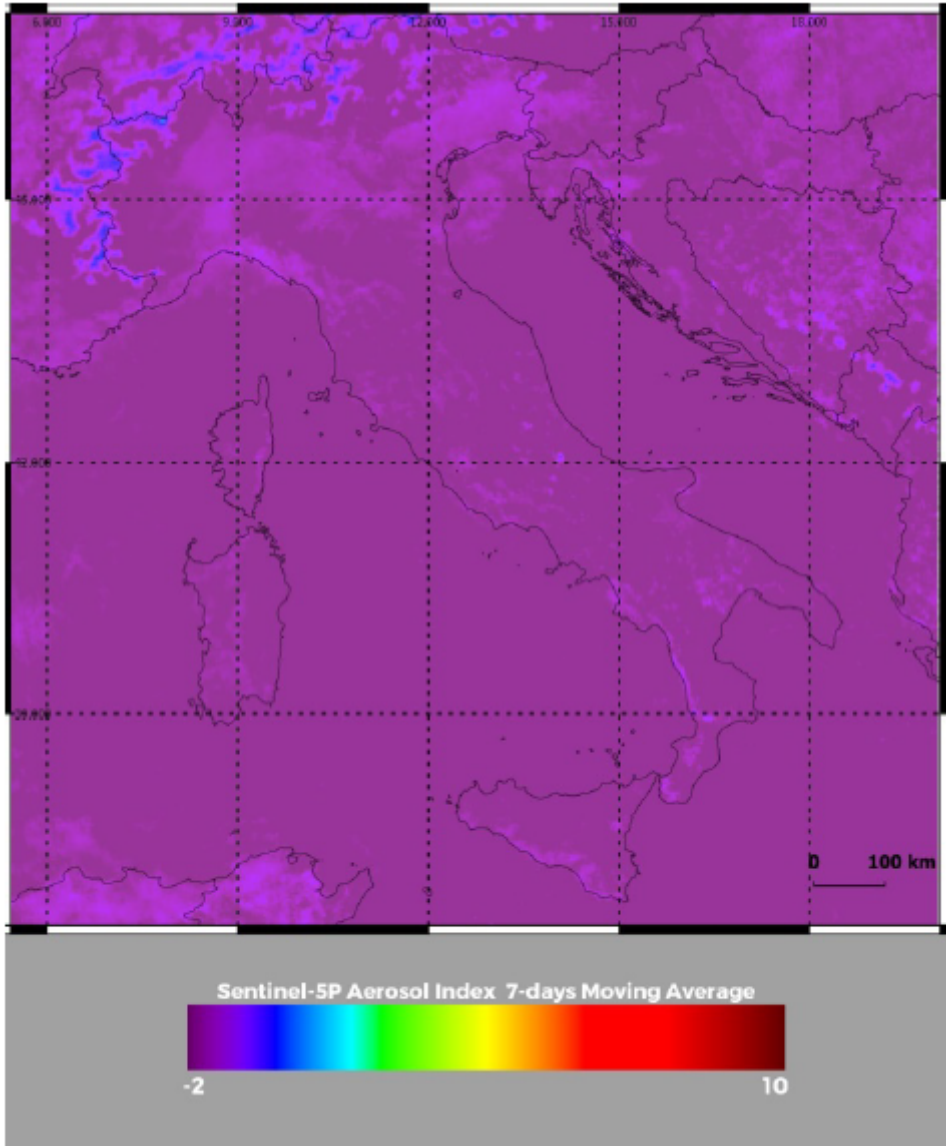


Figure 3

Aerosol index at 12:30 UTC on 17 February 2020 from Copernicus Sentinel-5P TROPOMI data over an area extending over the latitudinal interval 36-48° N and the longitudinal interval 5-20° E.

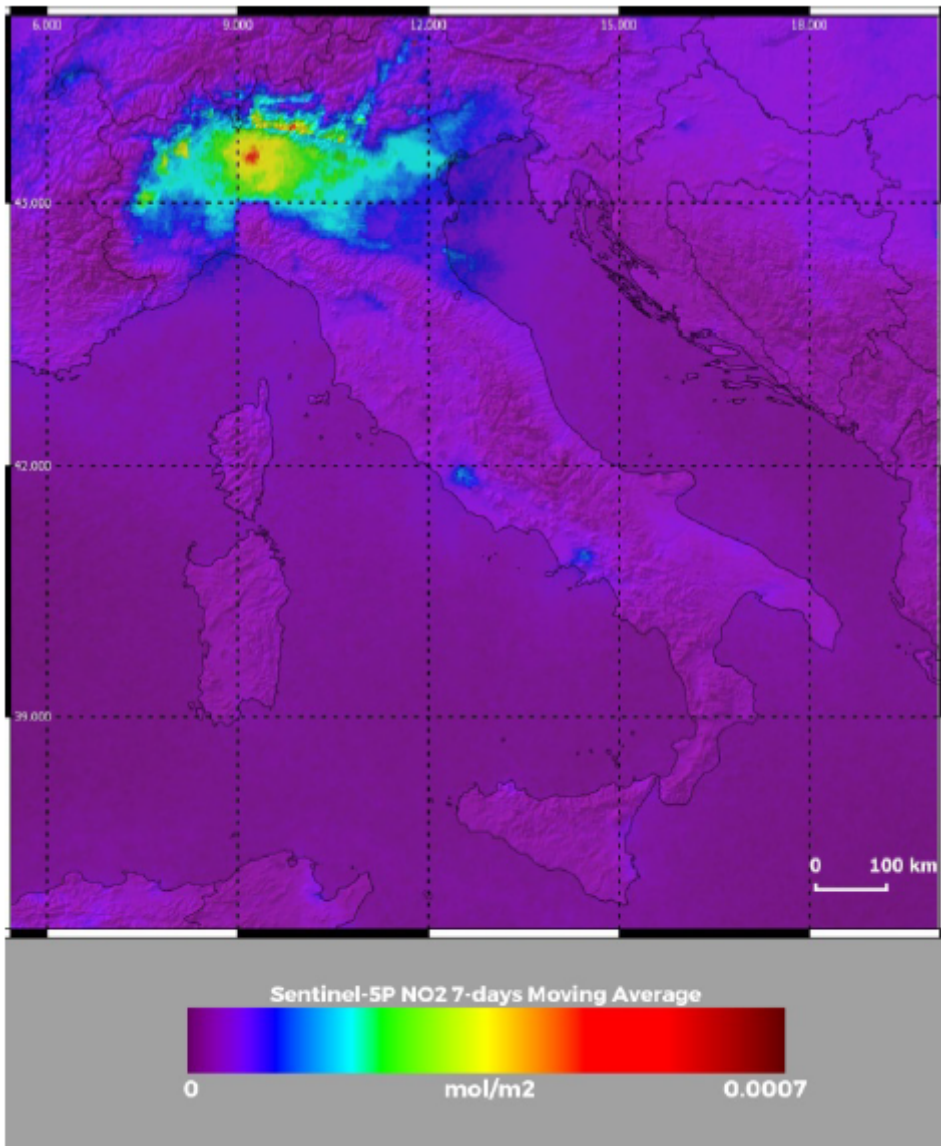


Figure 4

NO₂ concentration levels at 12:30 UTC on 17 February 2020 from Copernicus Sentinel- 5P TROPOMI data over an area extending over the latitudinal interval 36-48° N and the longitudinal interval 5-20° E.

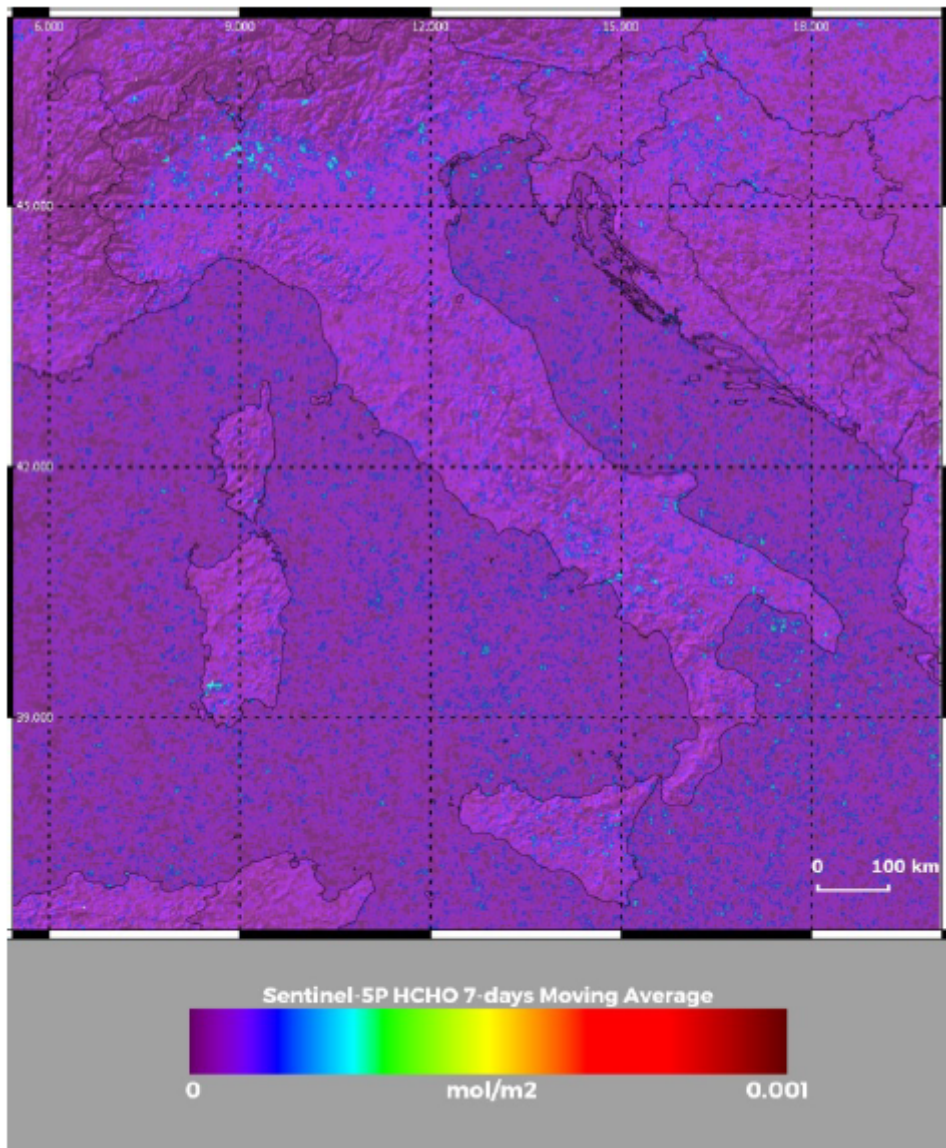


Figure 5

HCHO (formaldehyde) concentration levels at 12:30 UTC on 17 February 2020 from Copernicus Sentinel-5P TROPOMI data over an area extending over the latitudinal interval 36-48° N and the longitudinal interval 5-20° E.

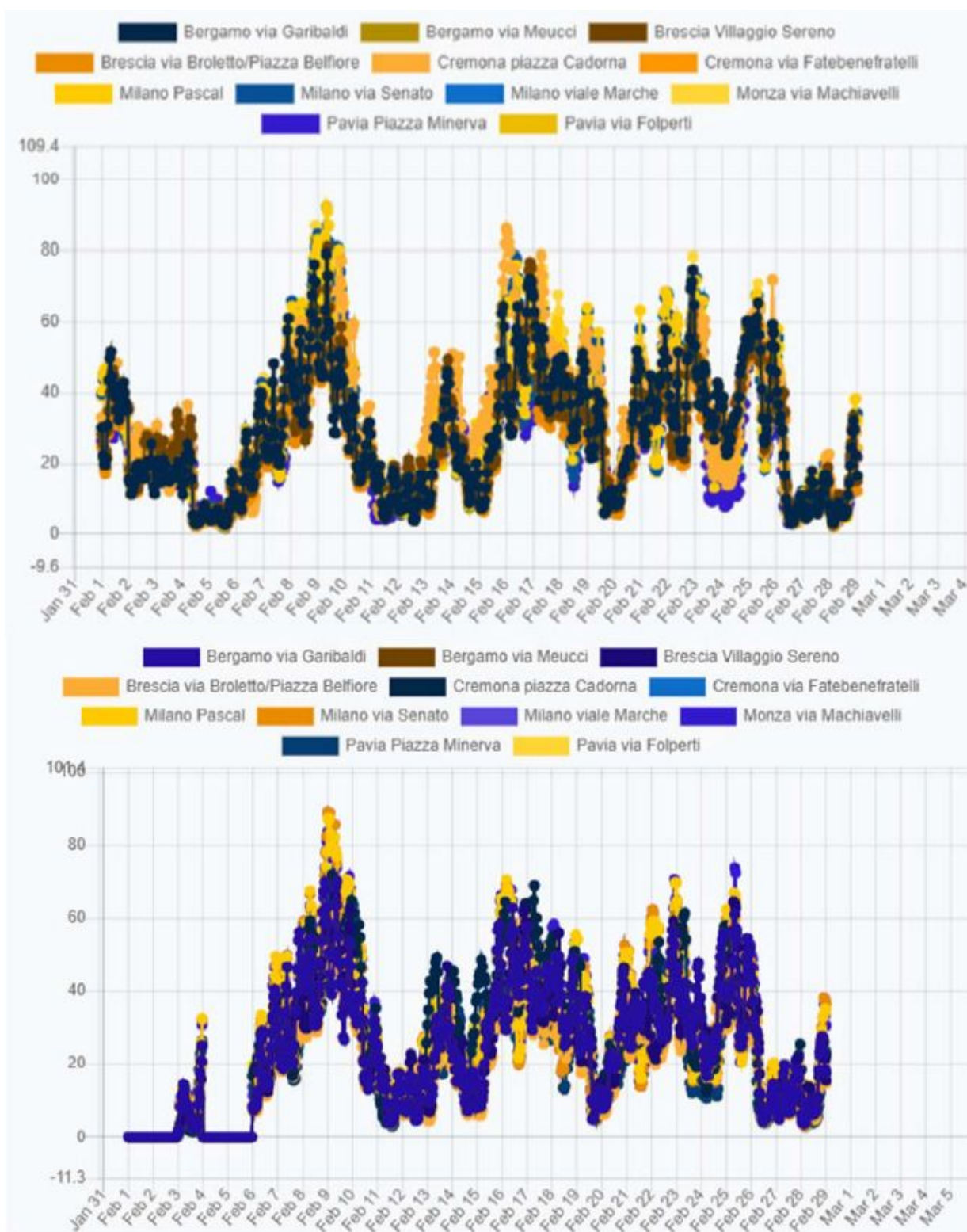


Figure 6

Near-real-time ECMWF-CAMS analysis of PM_{2.5} (upper panel) and PM_{2.5} (lower panel) concentration levels over the month of February 2020 for several metropolitan cities in Lombardia (Bergamo, Brescia, Cremona, Milano, Monza and Pavia). One to three locations are considered for each city.

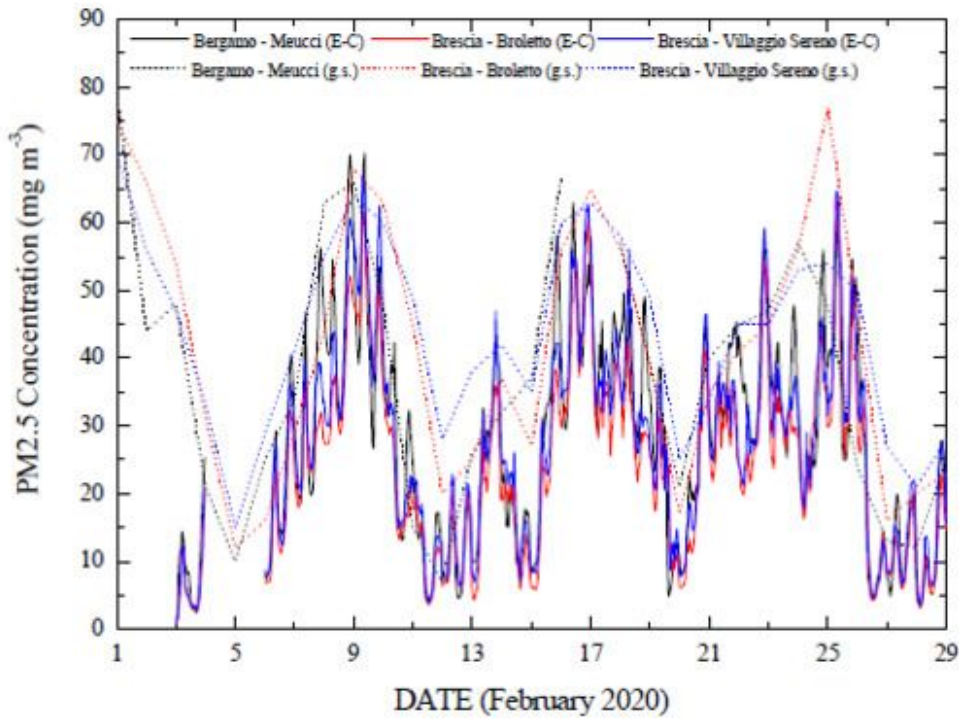
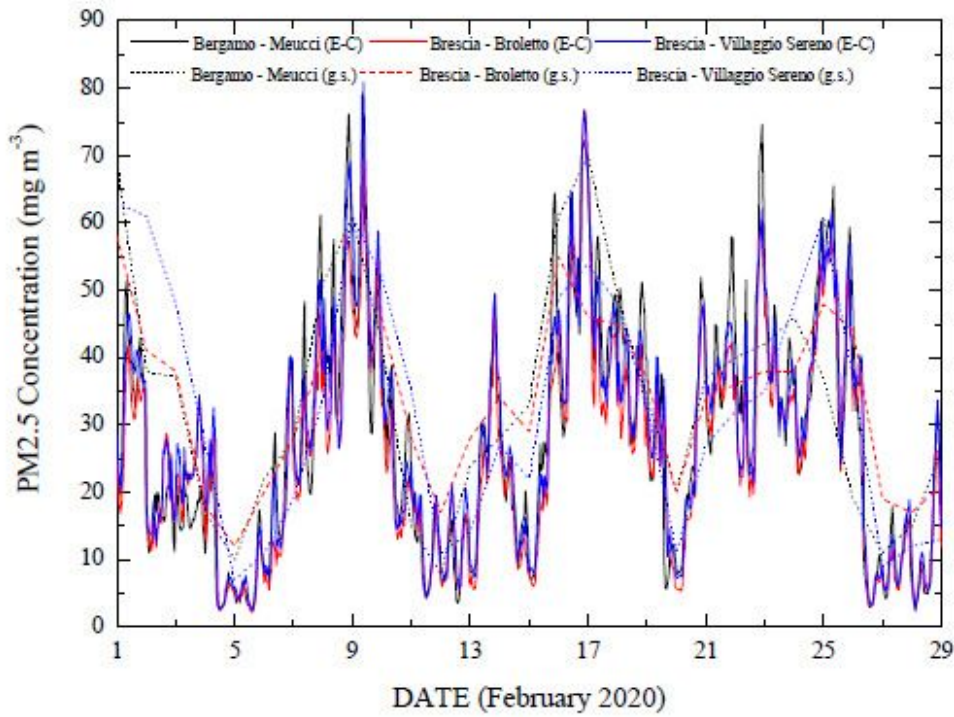


Figure 7

PM2.5 (upper panel) and PM10 (lower panel) concentration levels over month of February 2020 as measured by the three ground stations, one in Bergamo (via Meucci, 45°41'24" N, 09°38'28" E) and two in Brescia (via Broletto, 45°32'23" N, 10°13'24" E; Villaggio Sereno, 45°31'04" N, 10°10'41" E), together with the data from near-real-time ECMWF-CAMS analysis.

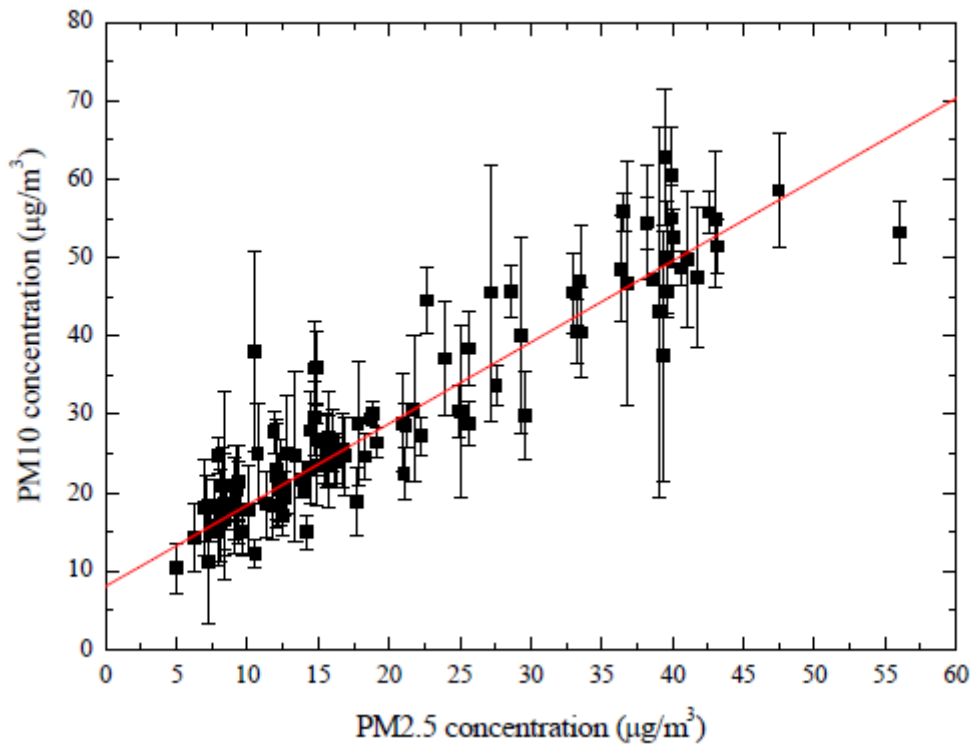


Figure 8

Scatter plot of mean PM10 vs PM2.5 concentration values over the period 15-26 February 2020.

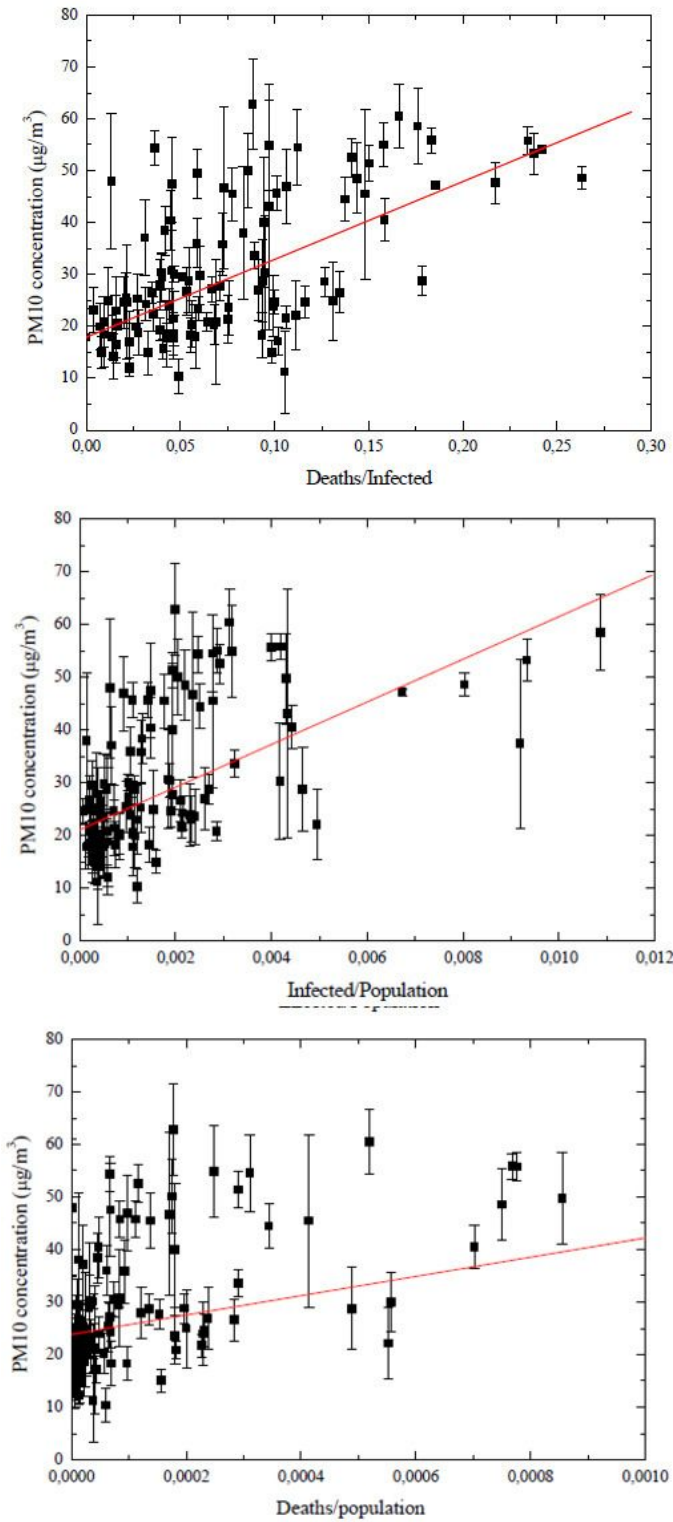


Figure 9

Linear regression analysis correlating the average PM10 concentration values in the period 15-26 February 2020 with the incidence of the pathology (upper panel), the mortality rate (middle panel) and the case fatality rate (lower panel) in the period 20 February-31 March 2020. The statistical analysis is extended over all 110 Italian Provinces.

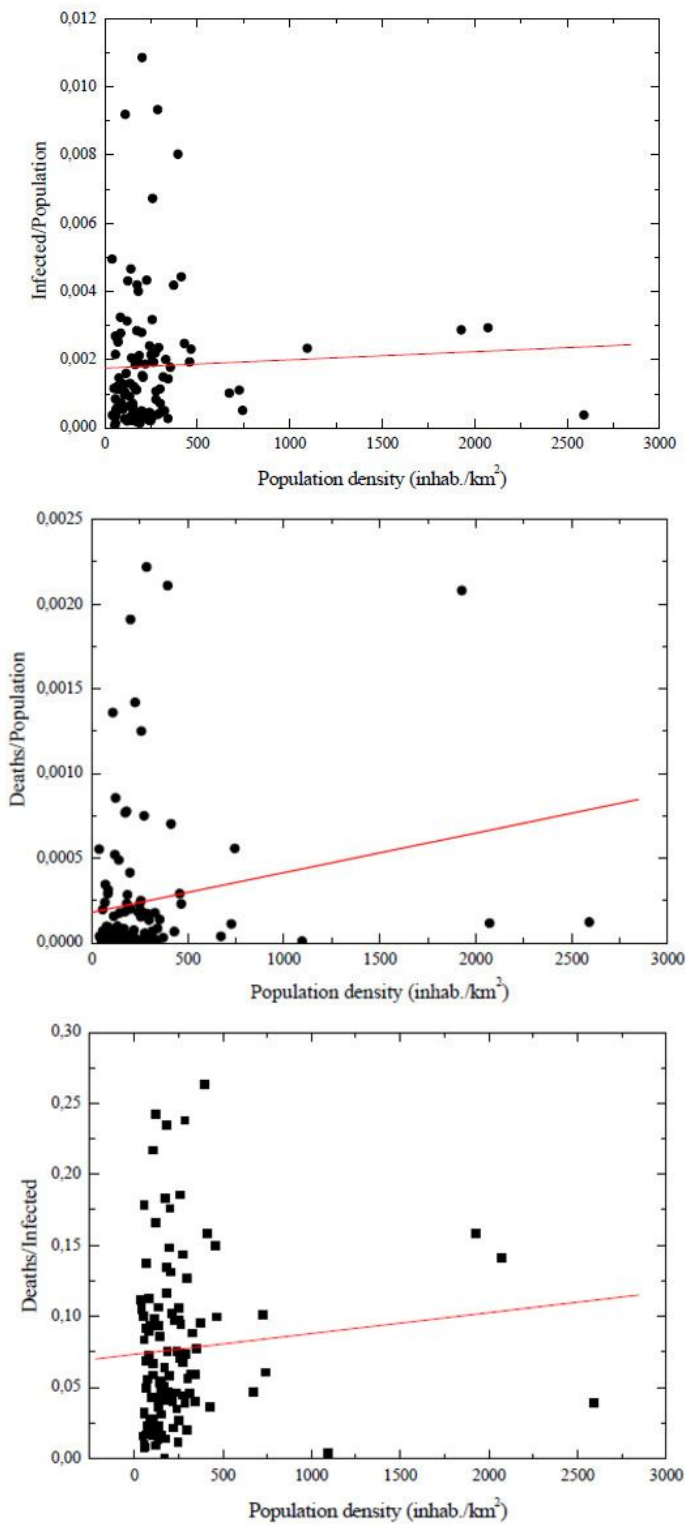


Figure 10

Linear regression analysis correlating population density with the incidence of the pathology (upper panel), the mortality rate (middle panel) and the case fatality rate (lower panel) in the period 20 February-31 March 2020. The statistical analysis is extended over all 110 Italian Provinces.